COMPUTER SIMULATION STUDIES OF SKYRMIONIC TEXTURES IN HELIMAGNETIC NANOSTRUCTURES

Marijan Beg*, Hans Fangohr

Faculty of Engineering and the Environment, **University of Southampton**, Southampton, United Kingdom

***email**: mb4e10@soton.ac.uk

OVERVIEW

1. Initial states (analytic model)
2. Equlibrium states in a nano disk
3. Ground state phase diagram
4. Robustness
5. Hysteretic behaviour (DMI anisotropy)
6. Reversal mechanism
7. Summary

SKYRMIONIC TEXTURES IN CONFINED HELIMAGNETIC NANOSTRUCTURES

MOTIVATION

- Magnetic skyrmions possess **interesting properties** promising for the development of future data-storage and information processing devices.
- One of the main problems, obstructing the development of skyrmion-based devices using helimagnetic materials, is their **magnetic** and **thermal stability**.
- In infinitely large thin film or bulk B20 helimagnetic samples, skyrmion phase is **stabilised in presence of an external field**.
- The motivation for this work is to **explore the skyrmionic textures in finite size B20 helimagnetic nanostructures**.

Yu et. al., Nature 465, 901-4 (2011)

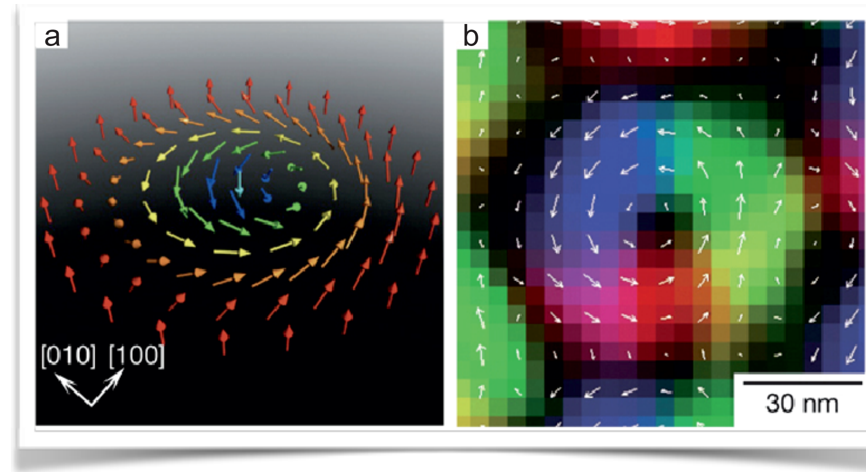

Schematic **Lorentz TEM**

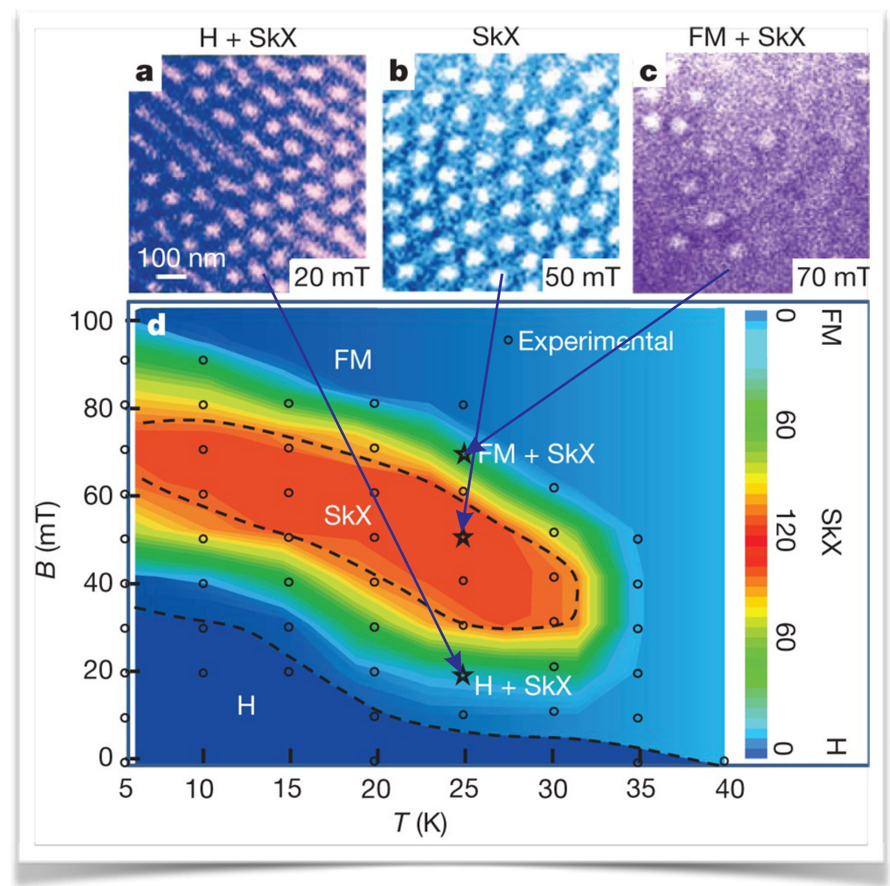

Thin film phase diagram

SYSTEM UNDER STUDY

- Sample geometry is **10 nm thin film disk** with varying diameter
- Cubic **B20 helimagnetic FeGe**
  - $M_S = 3.84 \times 10^5$ Am^{-1}
  - $A = 8.78 \times 10^{-12}$ Jm^{-1}
  - $D = 1.58 \times 10^{-3}$ Jm^{-2}.
  - Helical period $4\pi A/D = 70$ nm
- Finite elements mesh maximum neighbouring node spacing smaller than 3 nm.
- External field applied uniformly and **perpendicular to the film in +z direction**.
- zero temperature **micromagnetic model**

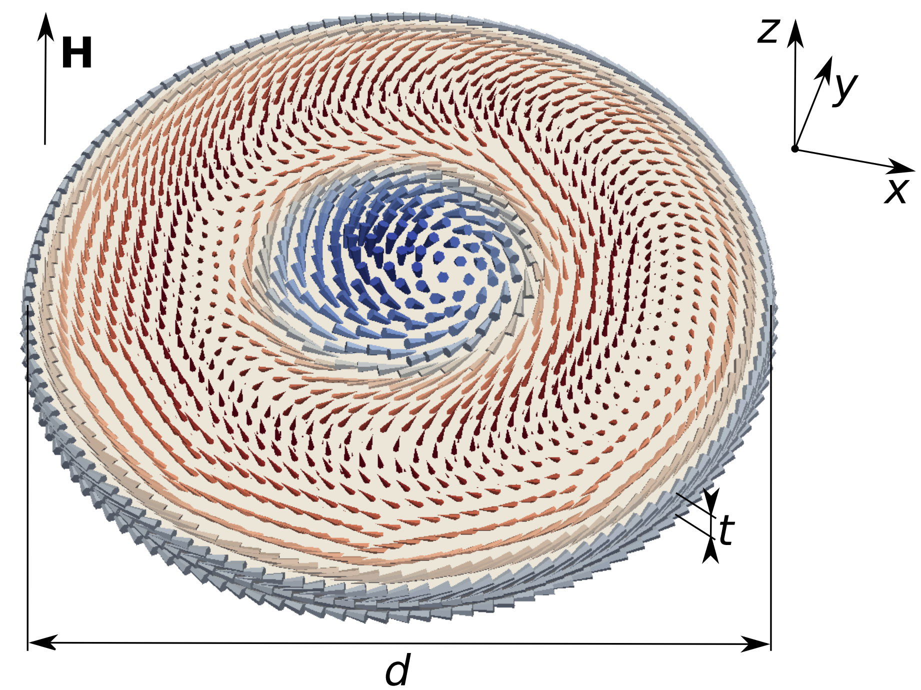

Sample geometry and sample skyrmion ground state

Finite size effects, stability, hysteretic behaviour, and reversal mechanism of skyrmionic textures in nanostructures,

Marijan Beg, Dmitri Chernyshenko, Marc-Antonio Bisotti, Weiwei Wang, Maximilian Albert, Robert L. Stamps, Hans Fangohr,

arxiv:1312.7665

http://arxiv.org/abs/1312.7665 (2014)

MICROMAGNETIC MODEL

- HAMILTONIAN AND DYNAMICS -

- **FINMAG**
  - Finite elements based simulator.
  - successor of Nmag, http://nmag.soton.ac.uk
- **HAMILTONIAN:**

$$W = \int \left[A(\nabla \mathbf{m})^2 + D\mathbf{m} \cdot (\nabla \times \mathbf{m}) - \mu_0 \mathbf{m} \cdot \mathbf{H} + w_\mathrm{d} \right] \mathrm{d}^3 r$$

  - **No anisotropy** (isotropic helimagnetic B20 material).
- **Full 3D model** - no assumption about translational invariance of magnetisation in out-of-film direction which radically changes the skyrmion energetics [Rybakov *et al.*, PRB **87**, 094424 (2013)].

MAGNETISATION DYNAMICS

- Magnetisation dynamics is governed by the **LLG EQUATION**.

$$\frac{\partial \mathbf{m}}{\partial t} = \underbrace{\gamma^* \mathbf{m} \times \mathbf{H}_{\mathrm{eff}}}_{\text{precession}} + \overbrace{\alpha \mathbf{m} \times \frac{\partial \mathbf{m}}{\partial t}}^{\text{damping}}$$

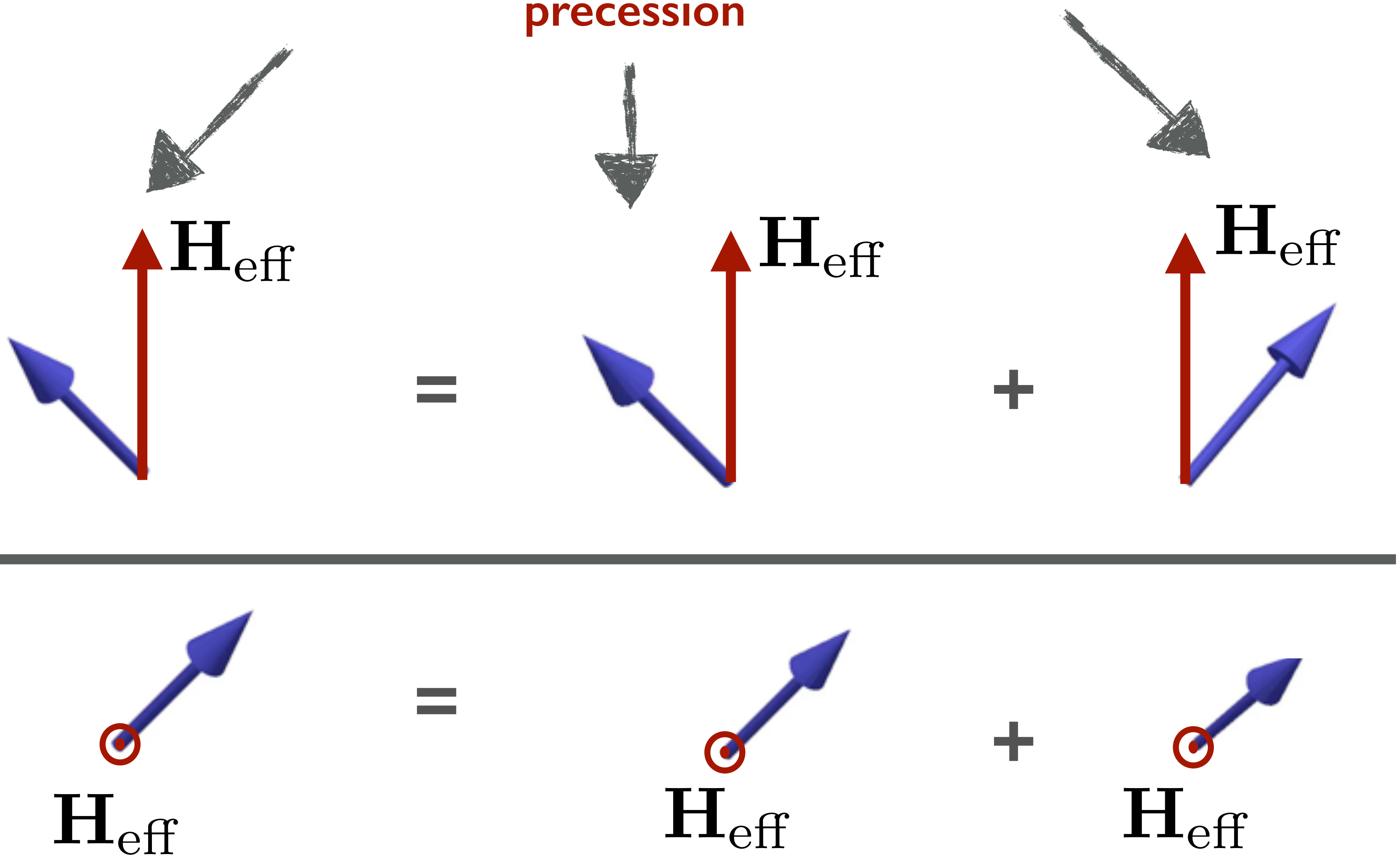

ENERGY LANDSCAPE

initial state

relaxed state

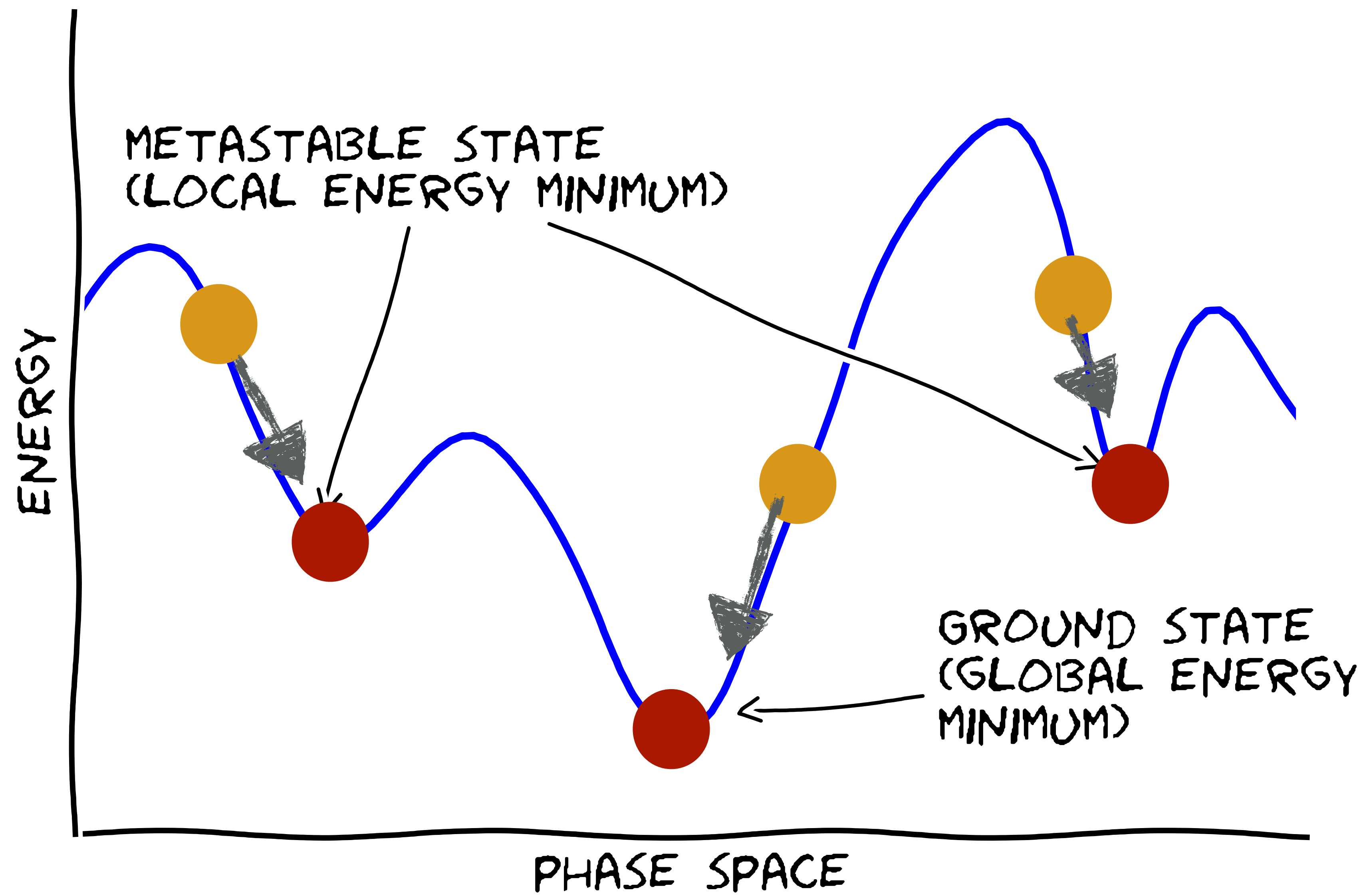

SIMULATION METHOD

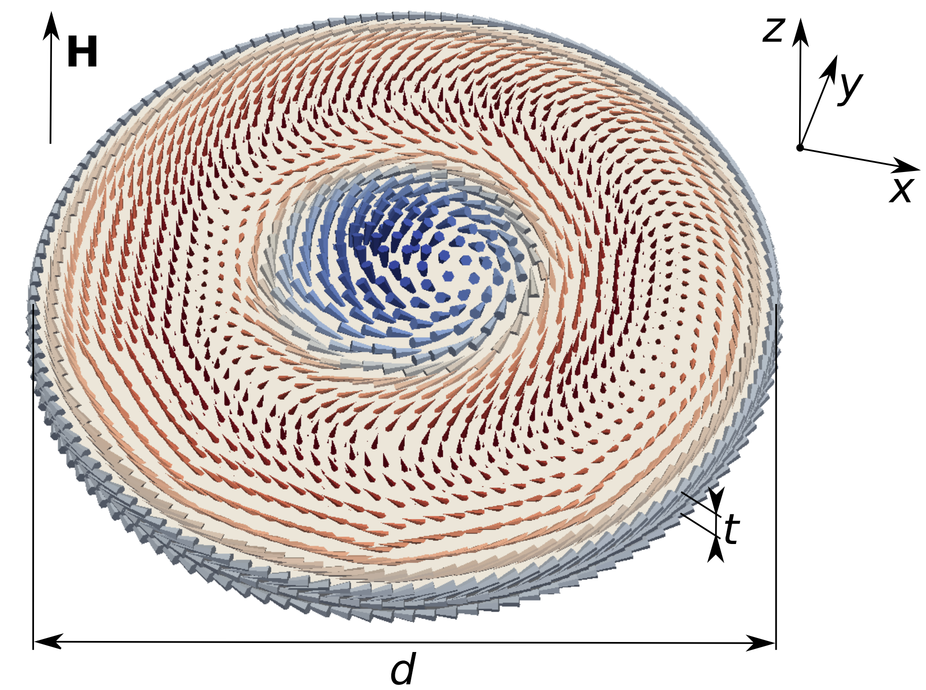

- ***d*** and ***H*** are **varied** in steps:

$$\Delta d = 2\,\mathrm{nm} \qquad \mu_0 \Delta H = 2\,\mathrm{mT}$$

- Gilbert damping $\alpha = 1$

- **System is relaxed** from **multiple initial states** by computing the magnetisation's time development
- The relaxed state with the lowest energy is chosen as the **ground state** for the phase space point (*d*, *H*).
- The **scalar parameter *S_a*** is computed as:

$$S_\mathrm{a} = \frac{1}{4\pi} \left| \mathbf{m} \cdot \left(\frac{\partial \mathbf{m}}{\partial x} \times \frac{\partial \mathbf{m}}{\partial x} \right) \right| \mathrm{d}^3 r$$

- **Phase diagram: S_a = *f*(*d*, *H*)**

INITIAL CONFIGURATIONS

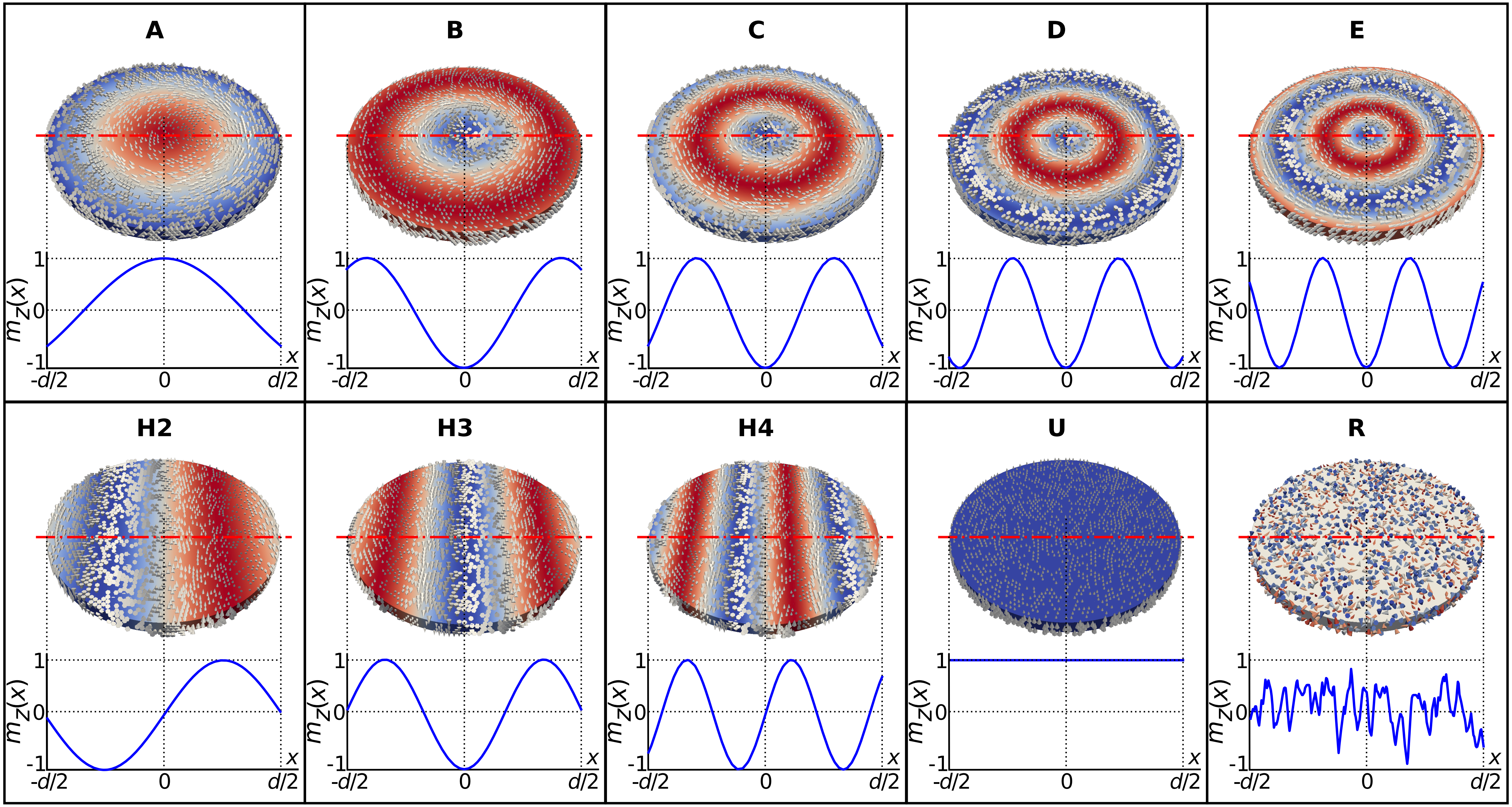

DEFINING SKYRMIONIC INITIAL STATES – ANALYTIC MODEL

- The **chiral skyrmion profile** is approximated in cylindrical coordinates:

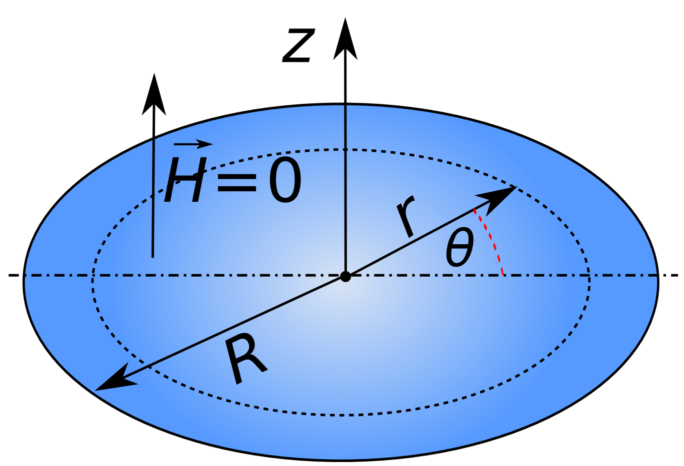

$$m_{\mathrm{r}} = 0$$

$$m_{\theta} = \sin(kr)$$

$$m_{\mathrm{z}} = -\cos(kr)$$

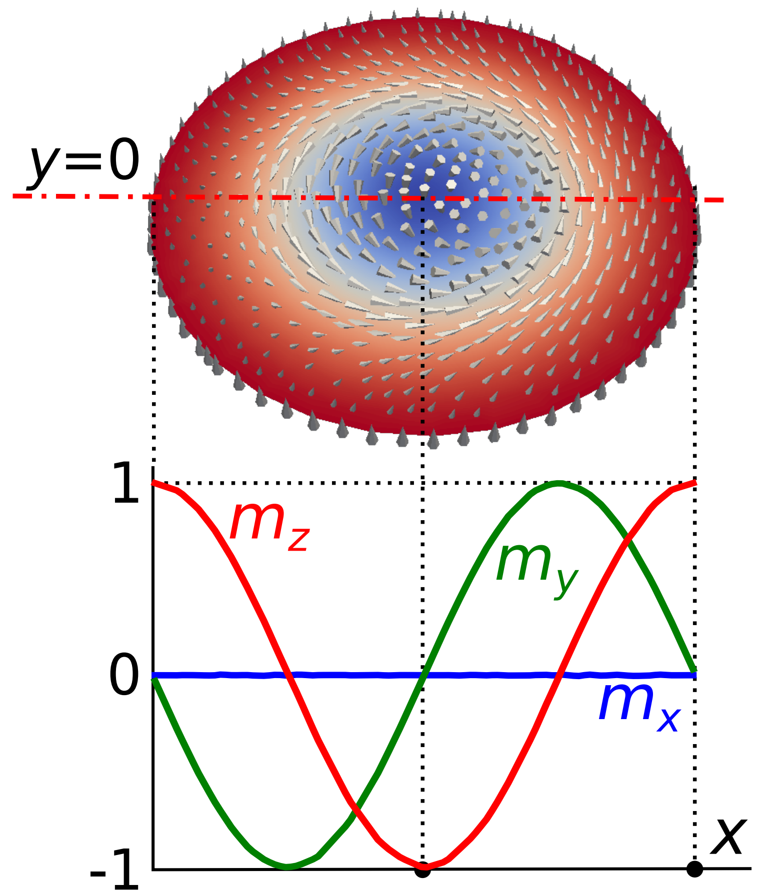

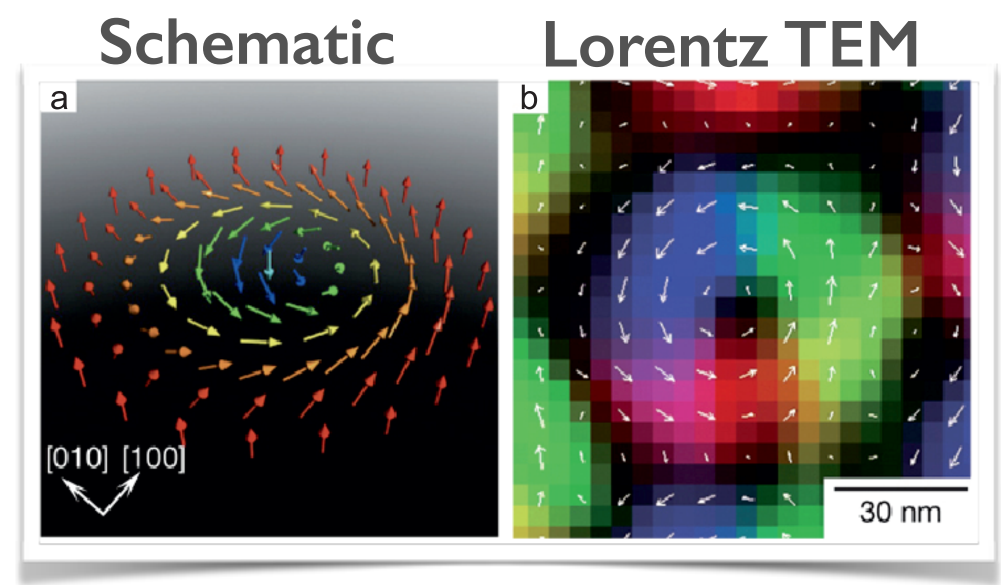

Yu et. al., Nature 465, 901-4 (2011)

- The **effective field** due to symmetric exchange and DMI (**no external field, isotropic B20 material**):

$$\vec{H}_{\mathrm{eff}} = -\frac{1}{\mu_0 M_{\mathrm{s}}} \frac{\delta w}{\delta \vec{m}}$$

$$\vec{H}_{\mathrm{eff}} = \frac{2}{\mu_0 M_{\mathrm{S}}} \left[A \nabla^2 \vec{m} - D (\nabla \times \vec{m}) \right]$$

ANALYTIC MODEL

- ZERO TORQUE EQUATION -

- In equilibrium state, the **torque is zero:** $\mathbf{m} \times \mathbf{H}_{\text{eff}} = 0$
- Computing the **zero radial torque at r=R** for assumed chiral skyrmion profile results in condition:

$$g(kR) \equiv -\frac{D}{kA}\sin^2(kR) - \frac{\sin(2kR)}{2kR} + 1 = 0$$

- This equation **has solution if**:

$$P = \frac{D}{kA} > \frac{2}{3} \quad \Rightarrow \quad D > \frac{2}{3}kA$$

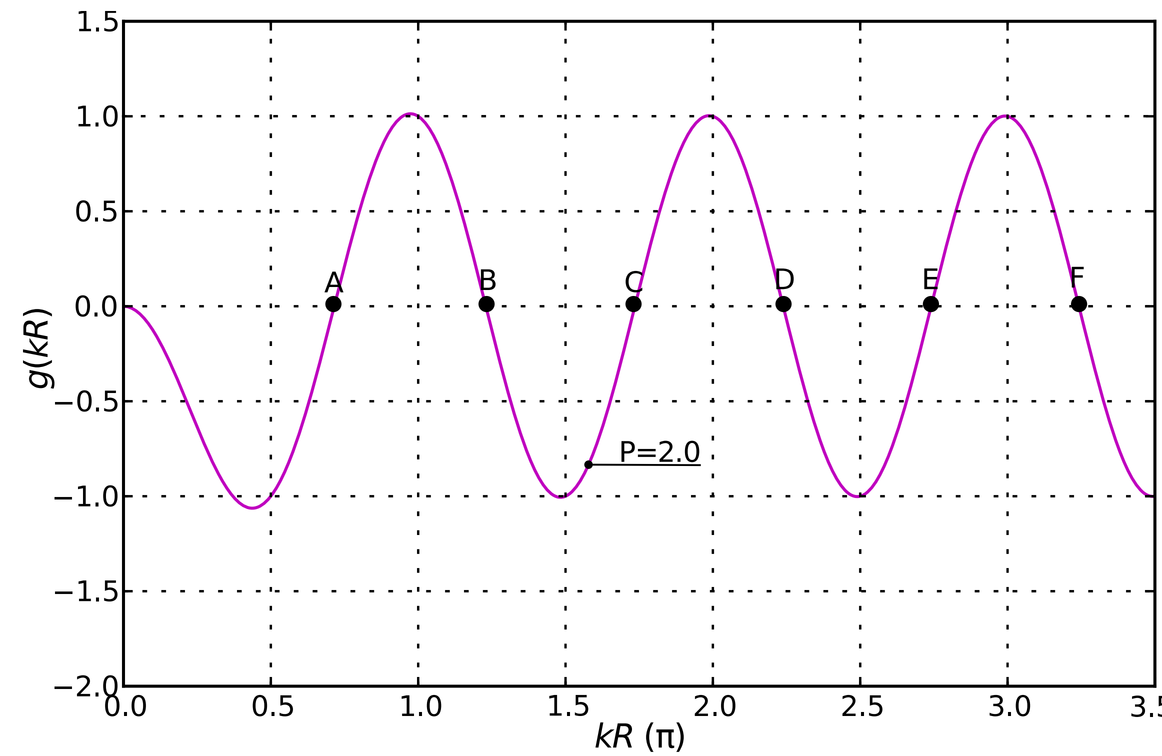

- Two scalar parameters are computed:

$$S = \int \mathbf{m} \cdot \left(\frac{\partial \mathbf{m}}{\partial x} \times \frac{\partial \mathbf{m}}{\partial y} \right) \mathrm{d}x\mathrm{d}y$$

$$S_{\mathrm{a}} = \int \left| \mathbf{m} \cdot \left(\frac{\partial \mathbf{m}}{\partial x} \times \frac{\partial \mathbf{m}}{\partial y} \right) \right| \mathrm{d}x\mathrm{d}y$$

$$m_{\mathrm{r}} = 0$$

$$m_{\theta} = \sin(kr)$$

$$m_{\mathrm{z}} = -\cos(kr)$$

SOLUTION A

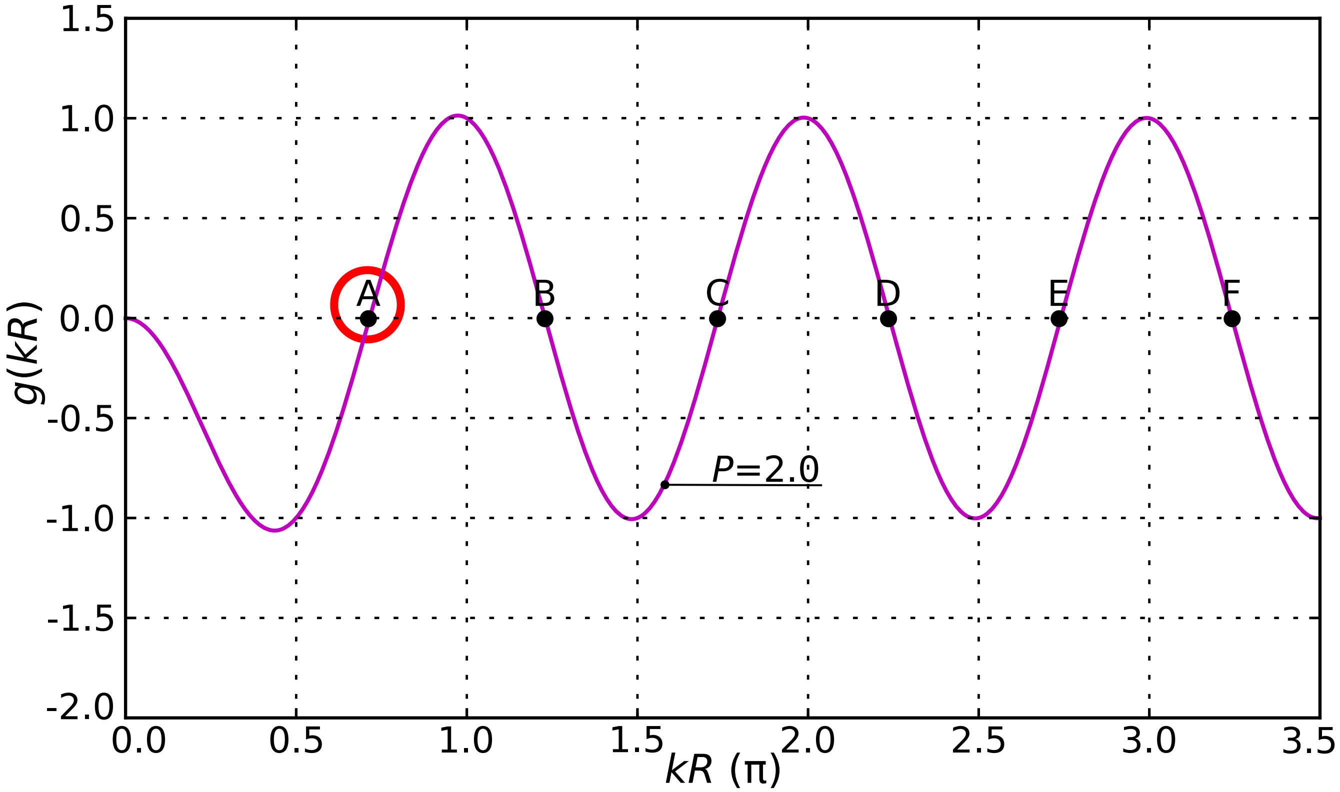

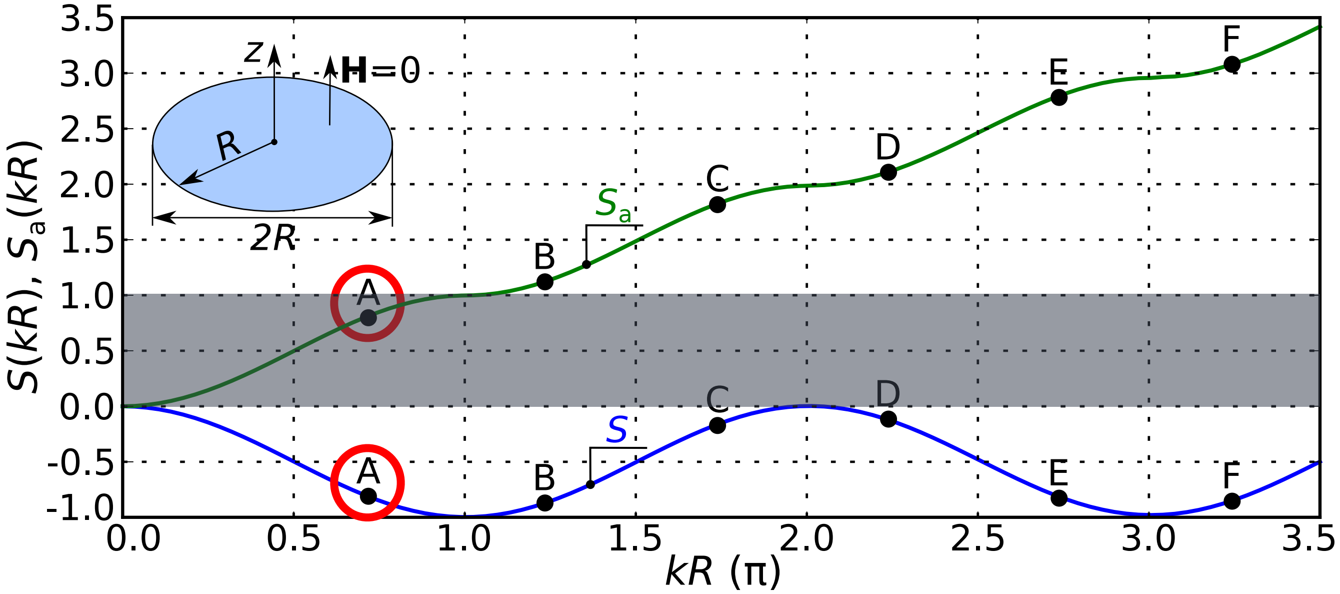

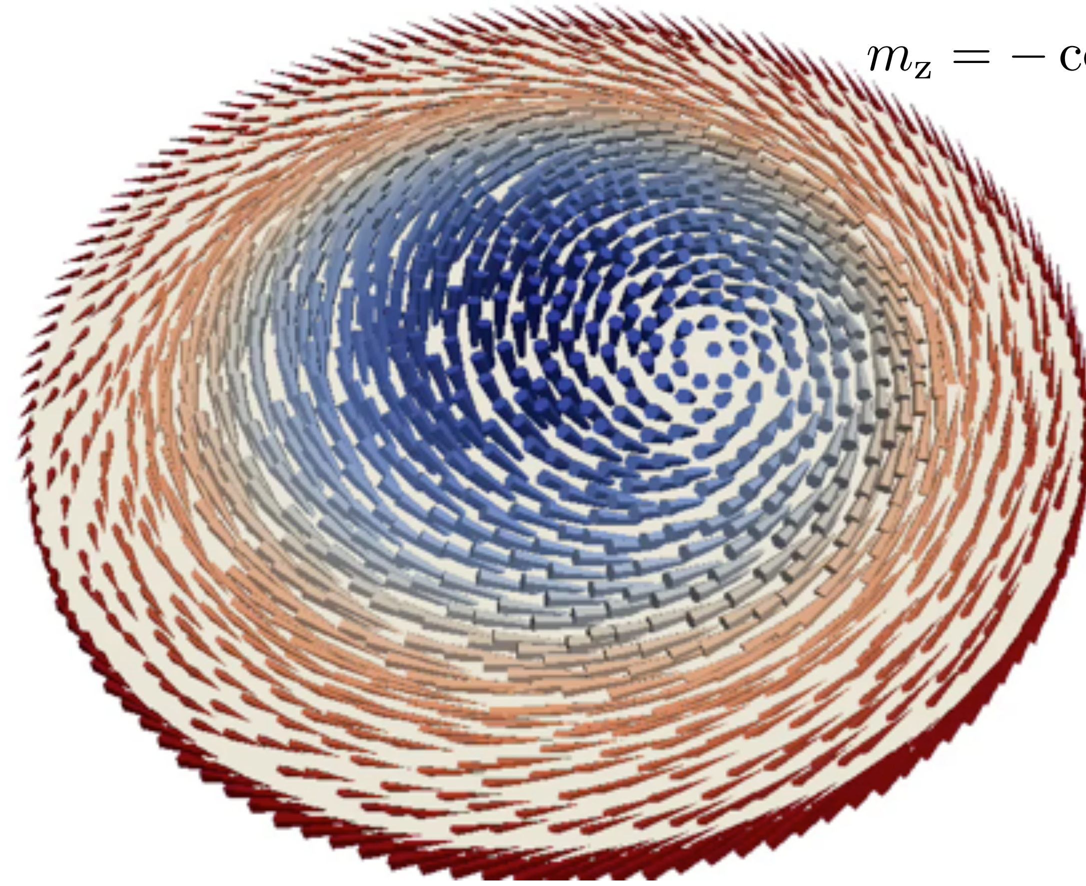

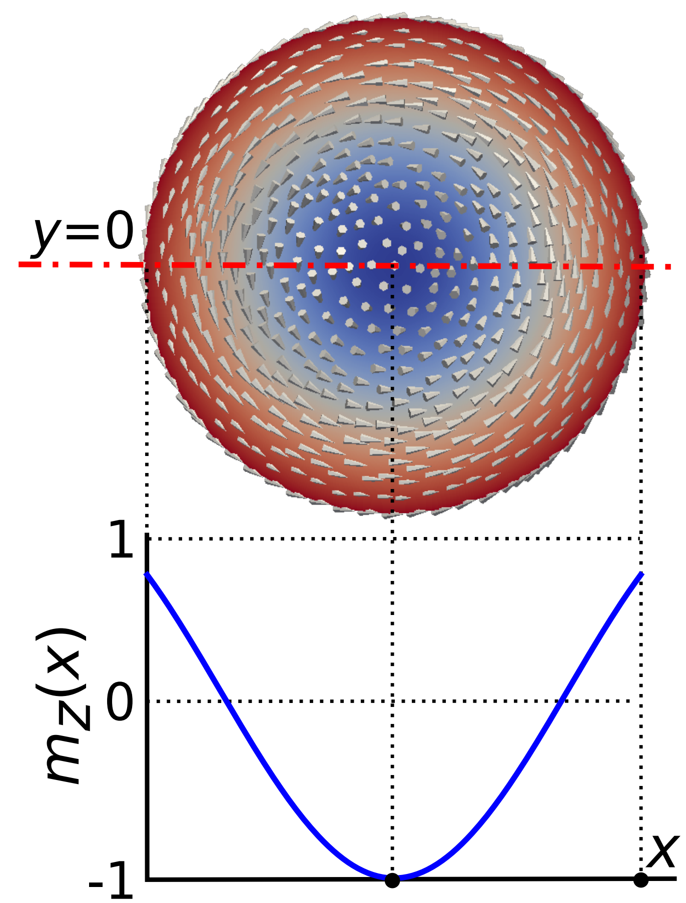

$$m_{\mathrm{r}} = 0$$

$$m_{\theta} = \sin(kr)$$

$$m_{\mathrm{z}} = -\cos(kr)$$

SOLUTION B

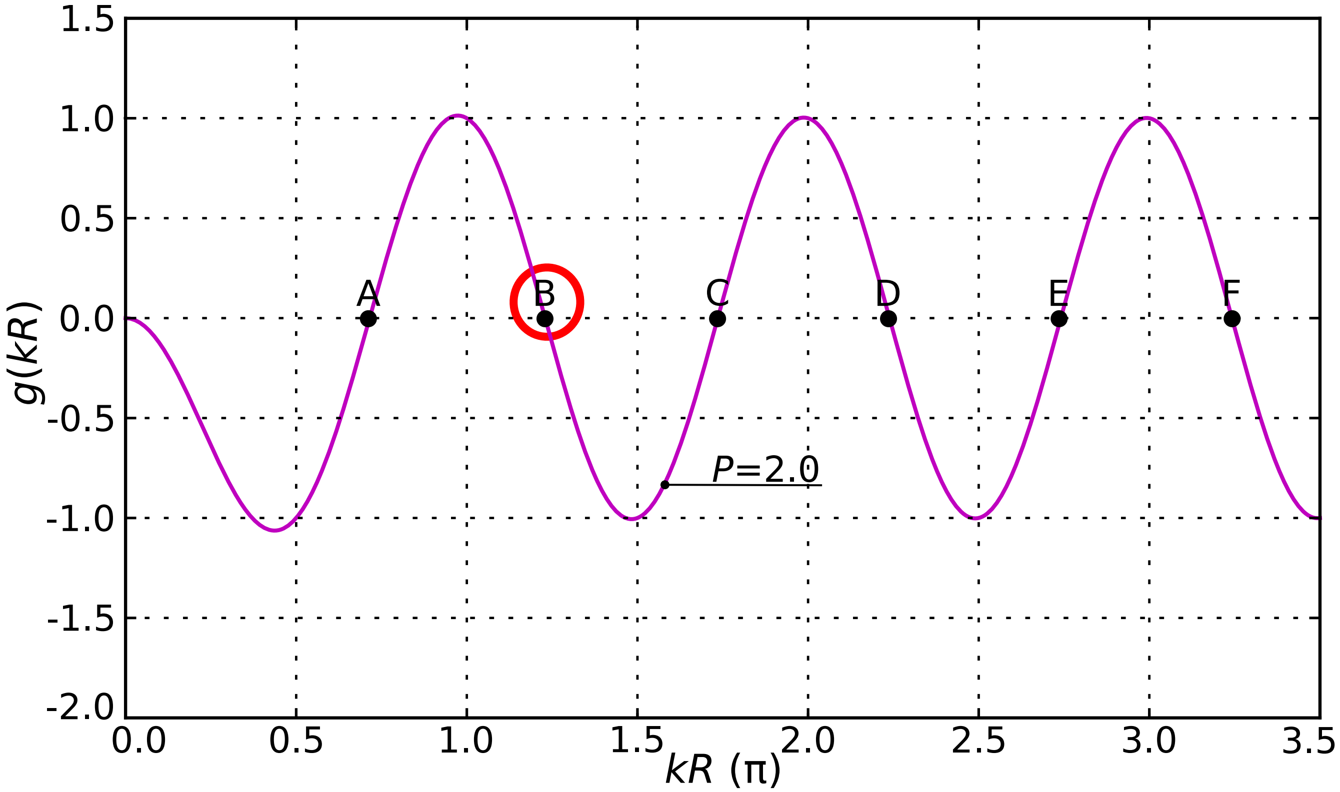

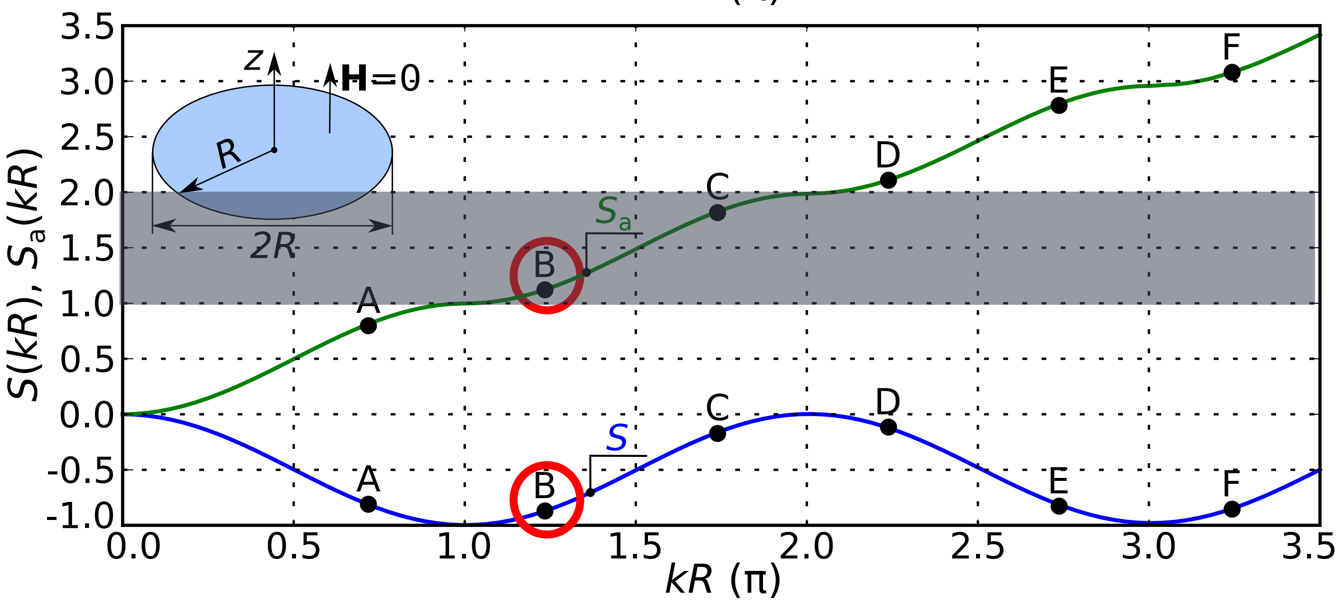

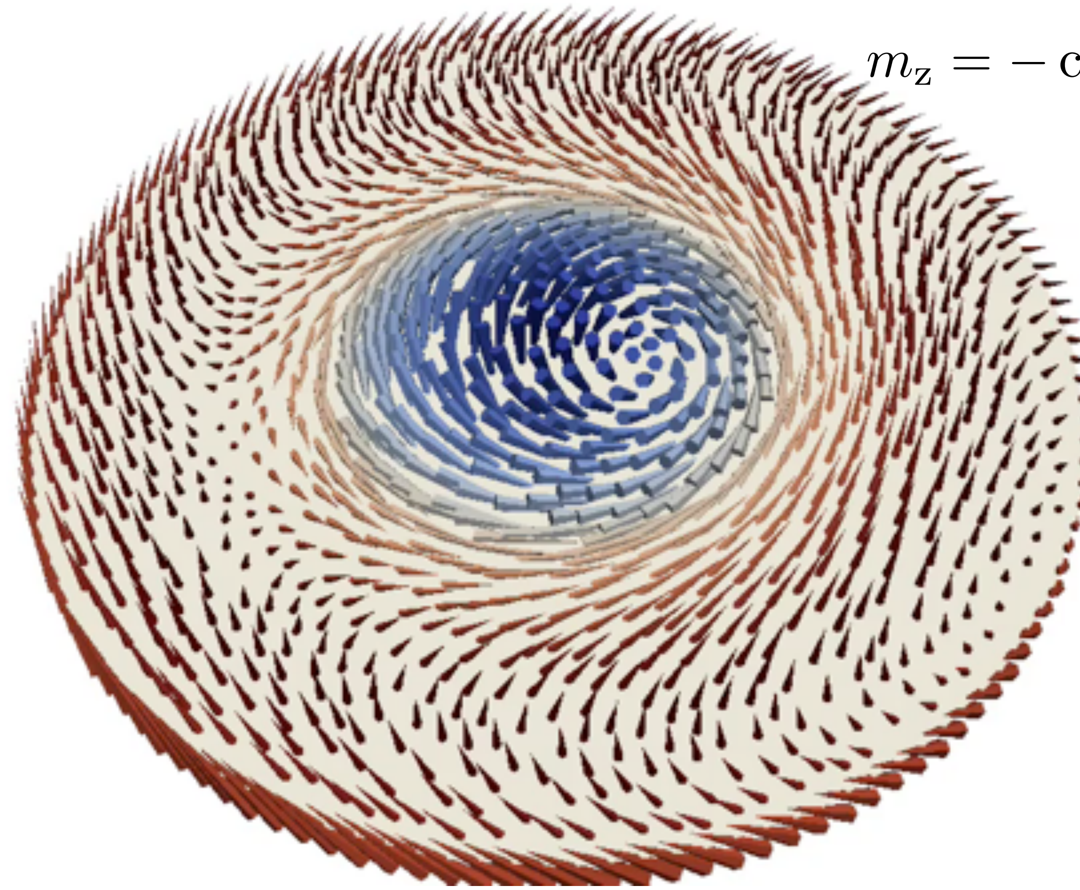

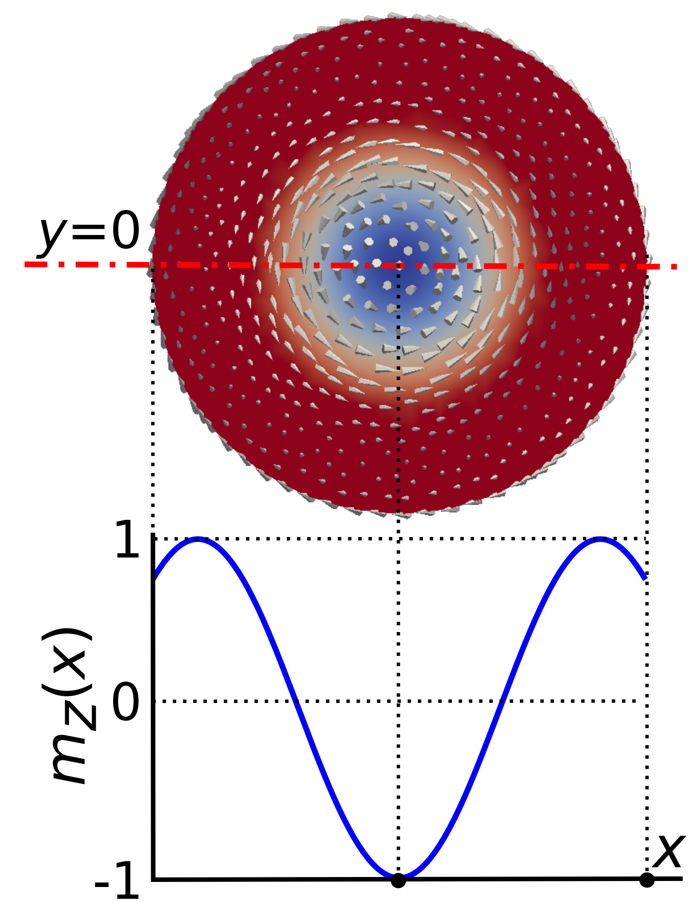

$$m_{\mathrm{r}} = 0$$

$$m_{\theta} = \sin(kr)$$

$$m_{\mathrm{z}} = -\cos(kr)$$

SOLUTION C

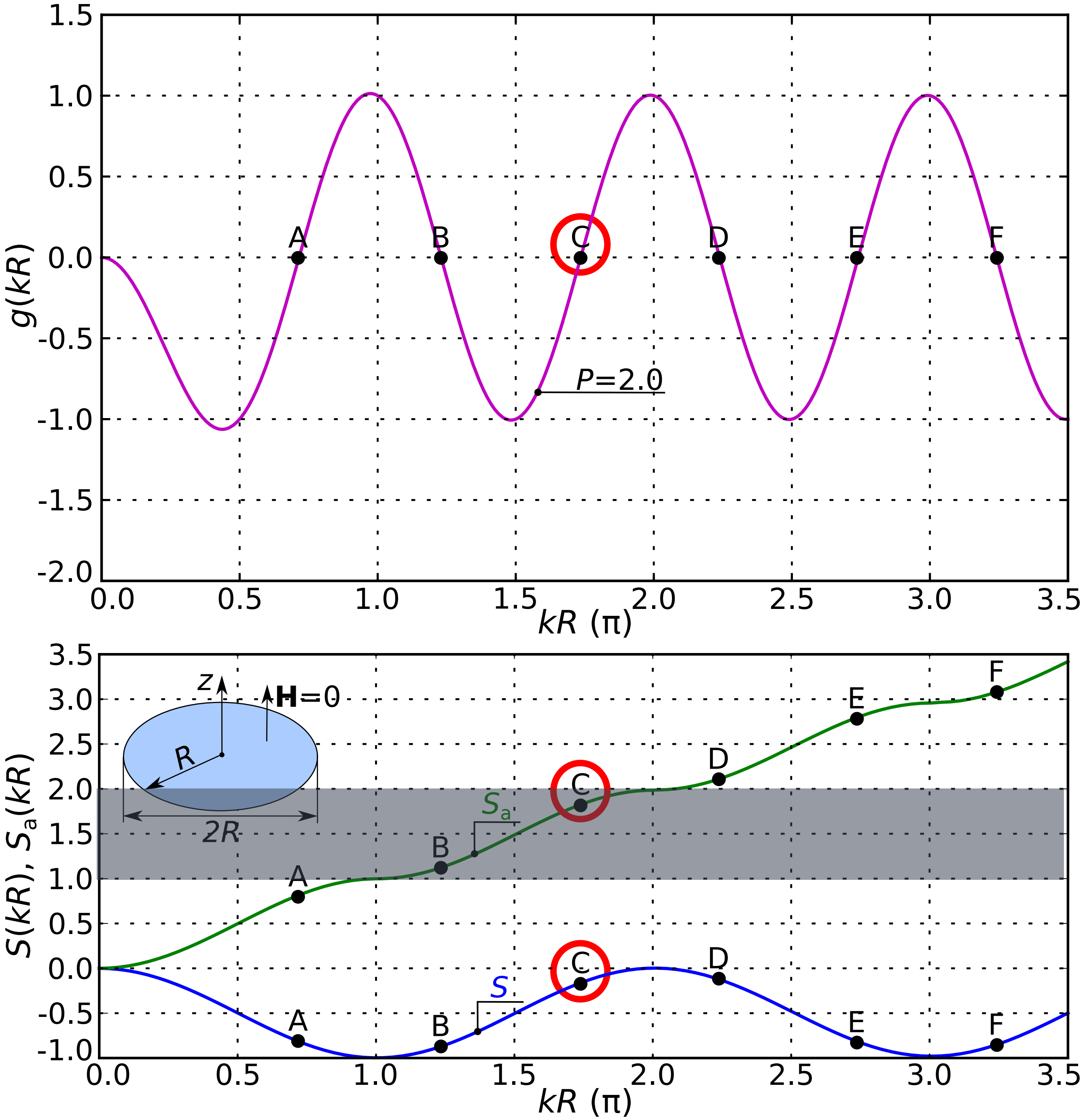

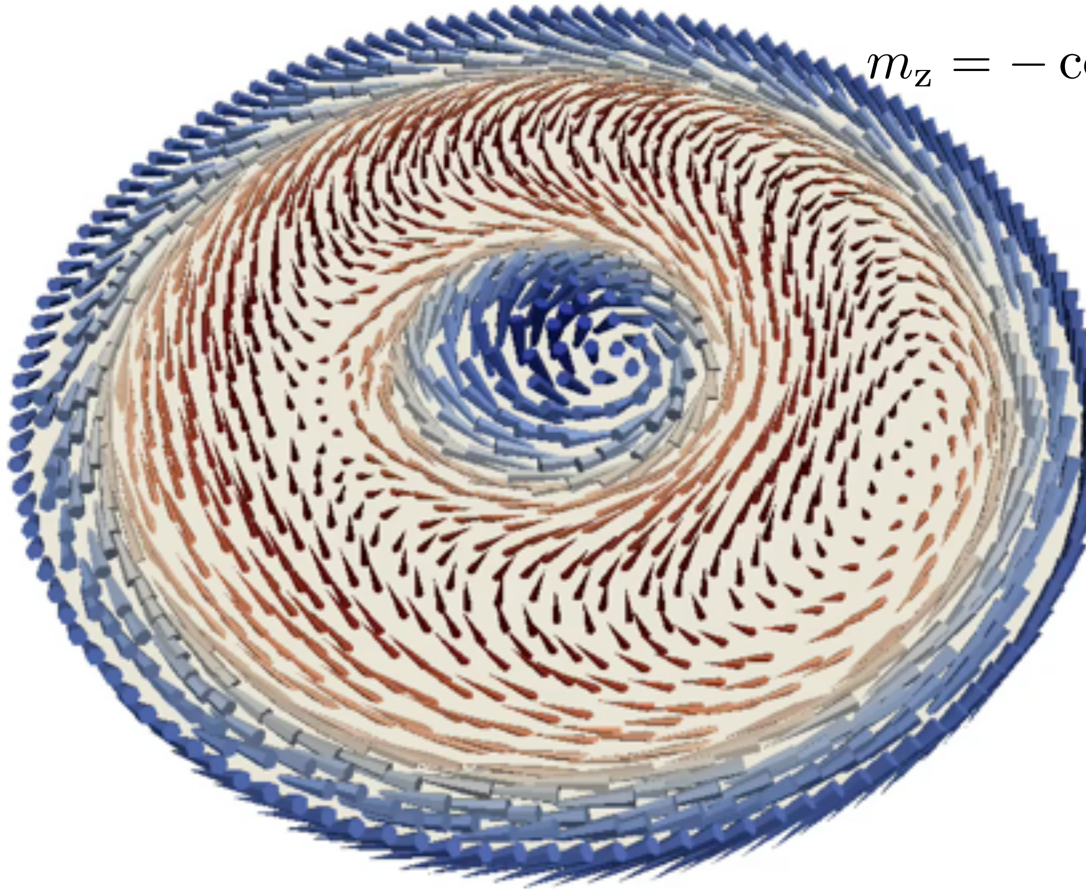

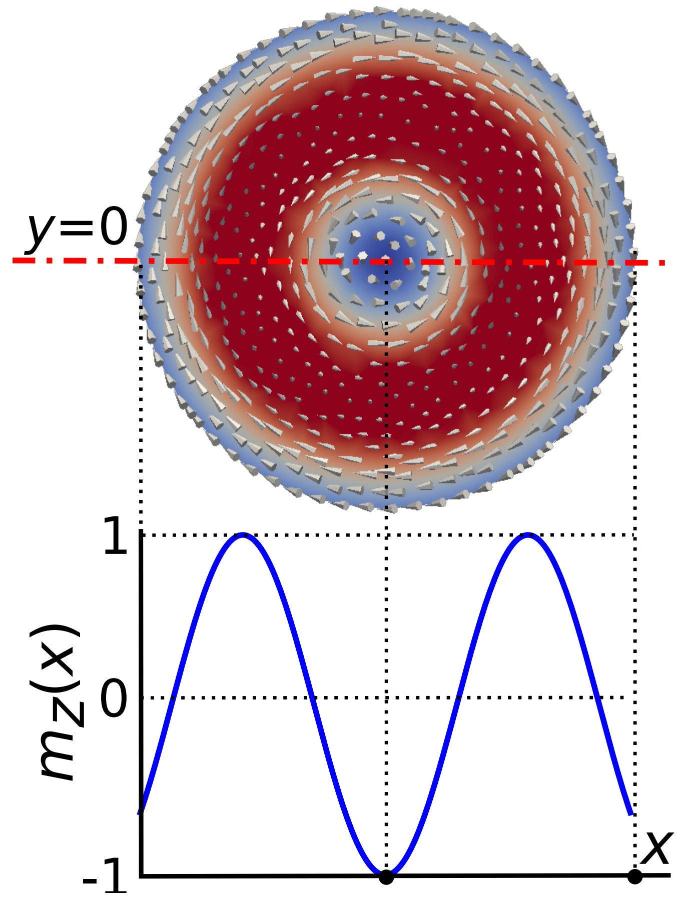

SOLUTION D

$$m_r = 0$$

$$m_\theta = \sin(kr)$$

$$m_z = -\cos(kr)$$

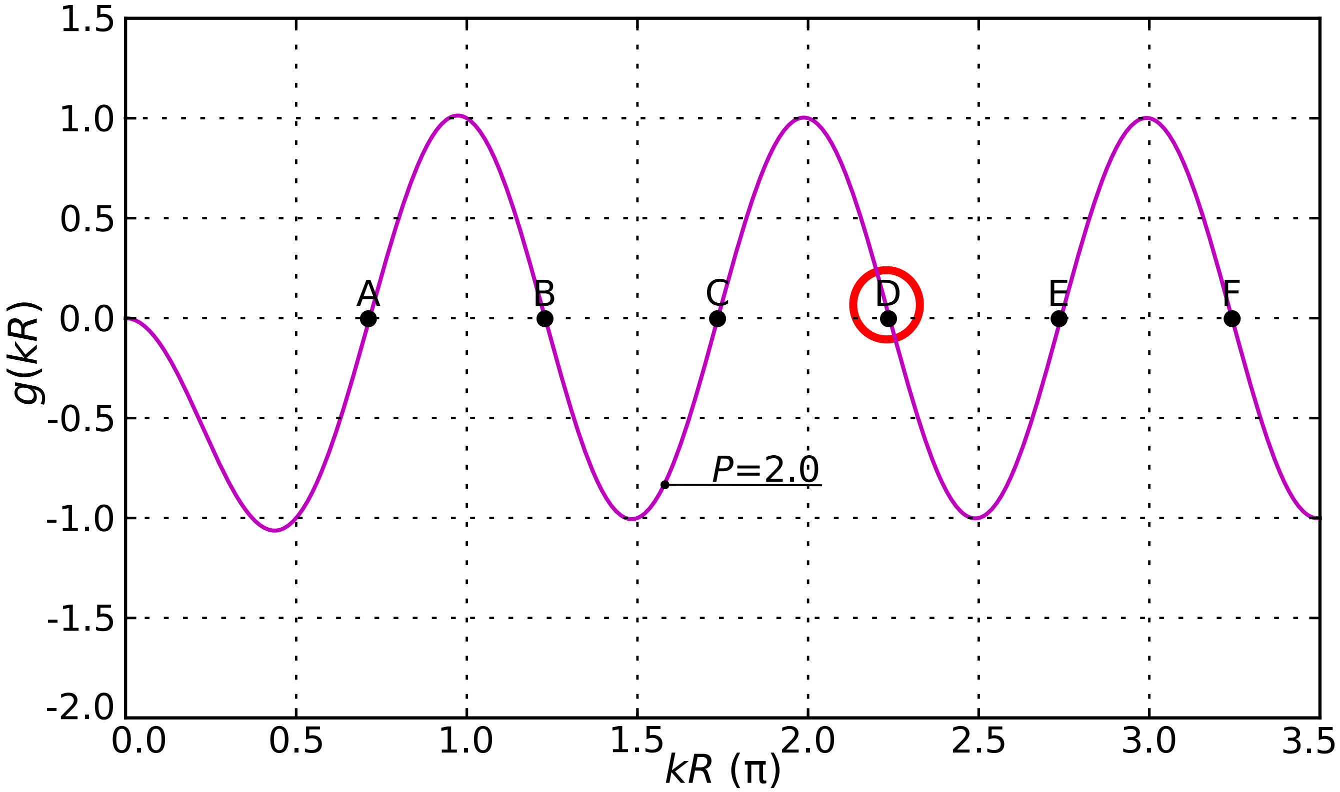

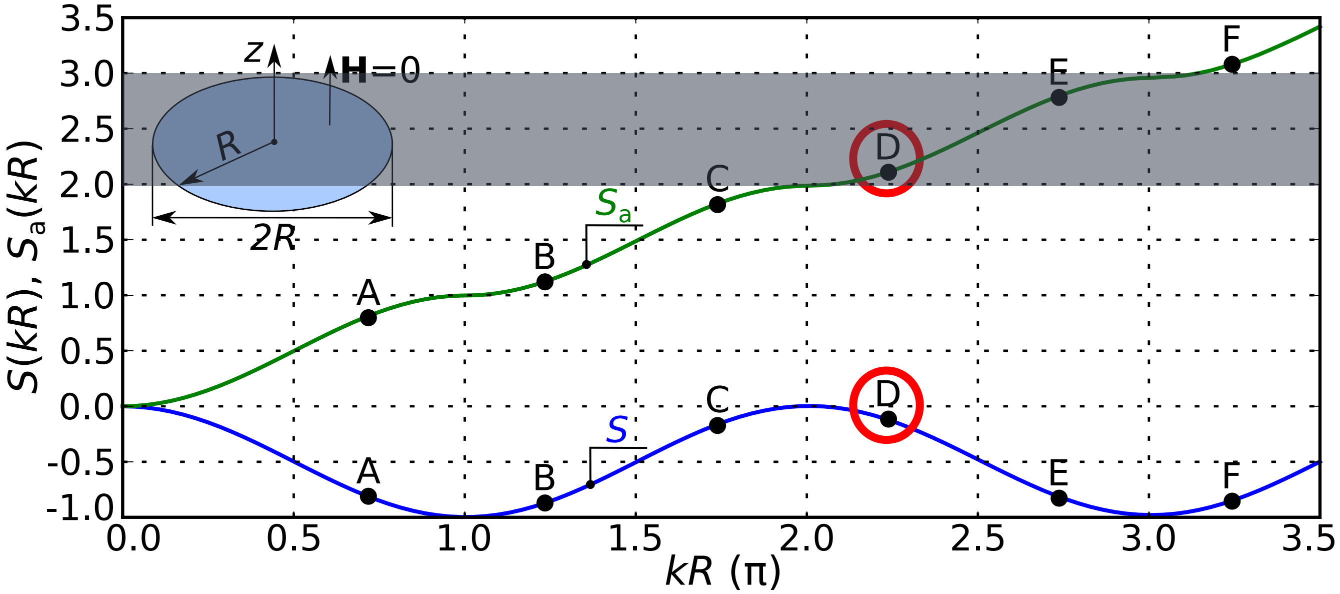

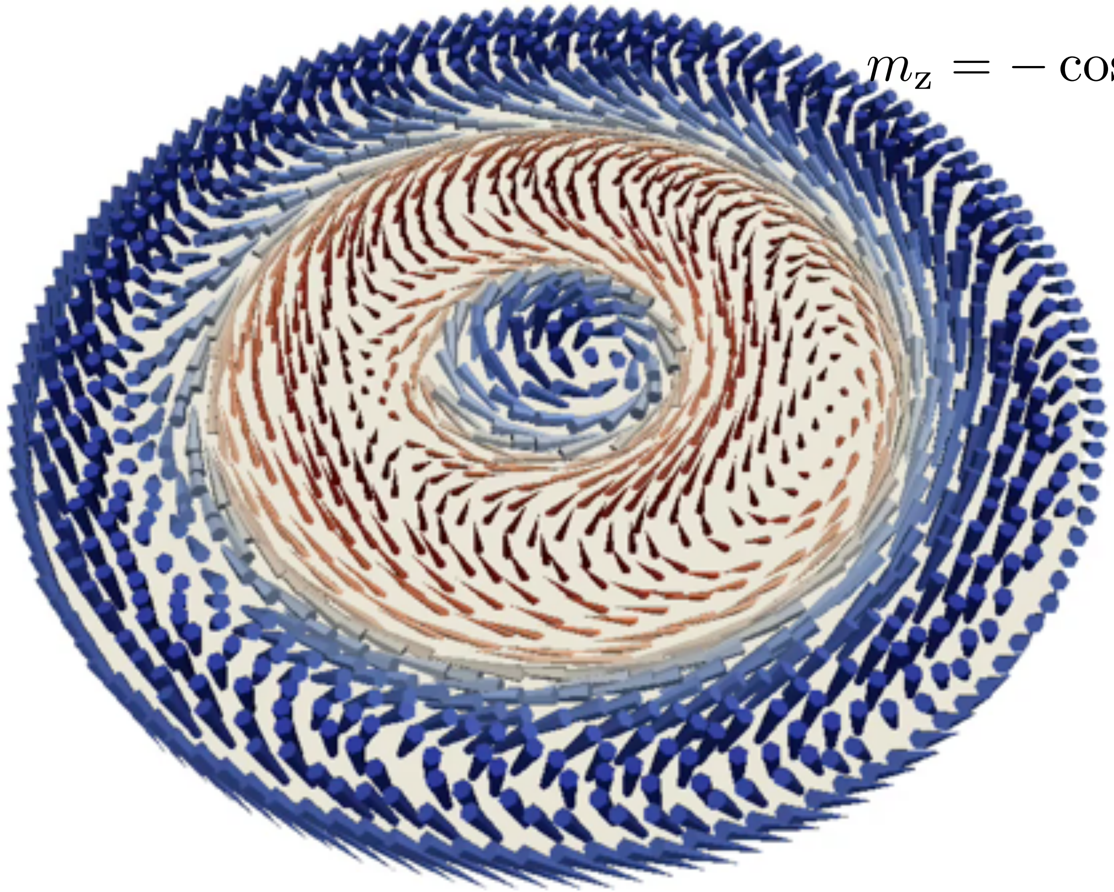

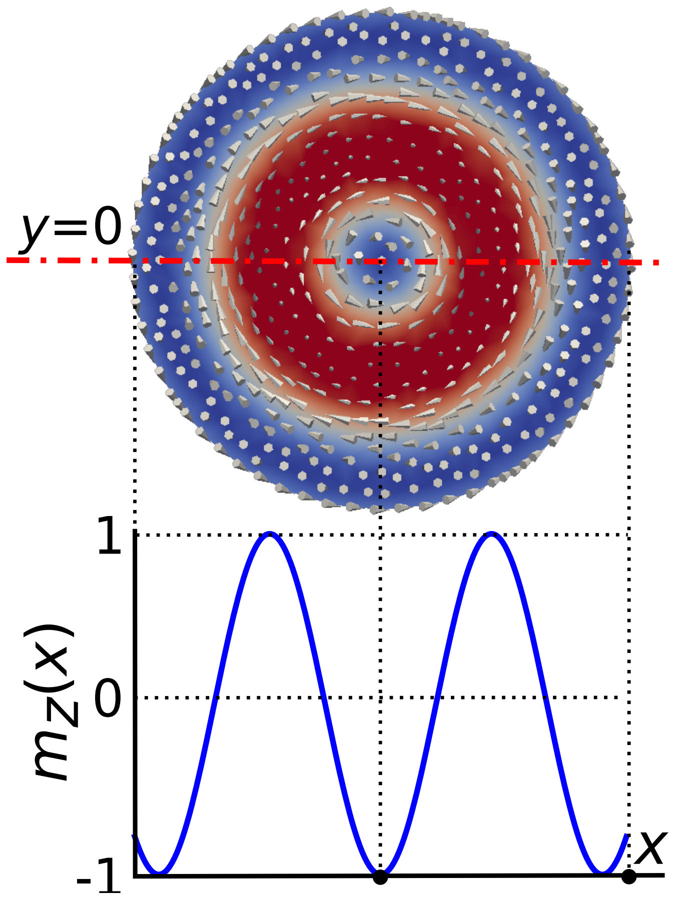

SOLUTION E

$$m_{\mathrm{r}} = 0$$
$$m_{\theta} = \sin(kr)$$
$$m_{\mathrm{z}} = -\cos(kr)$$

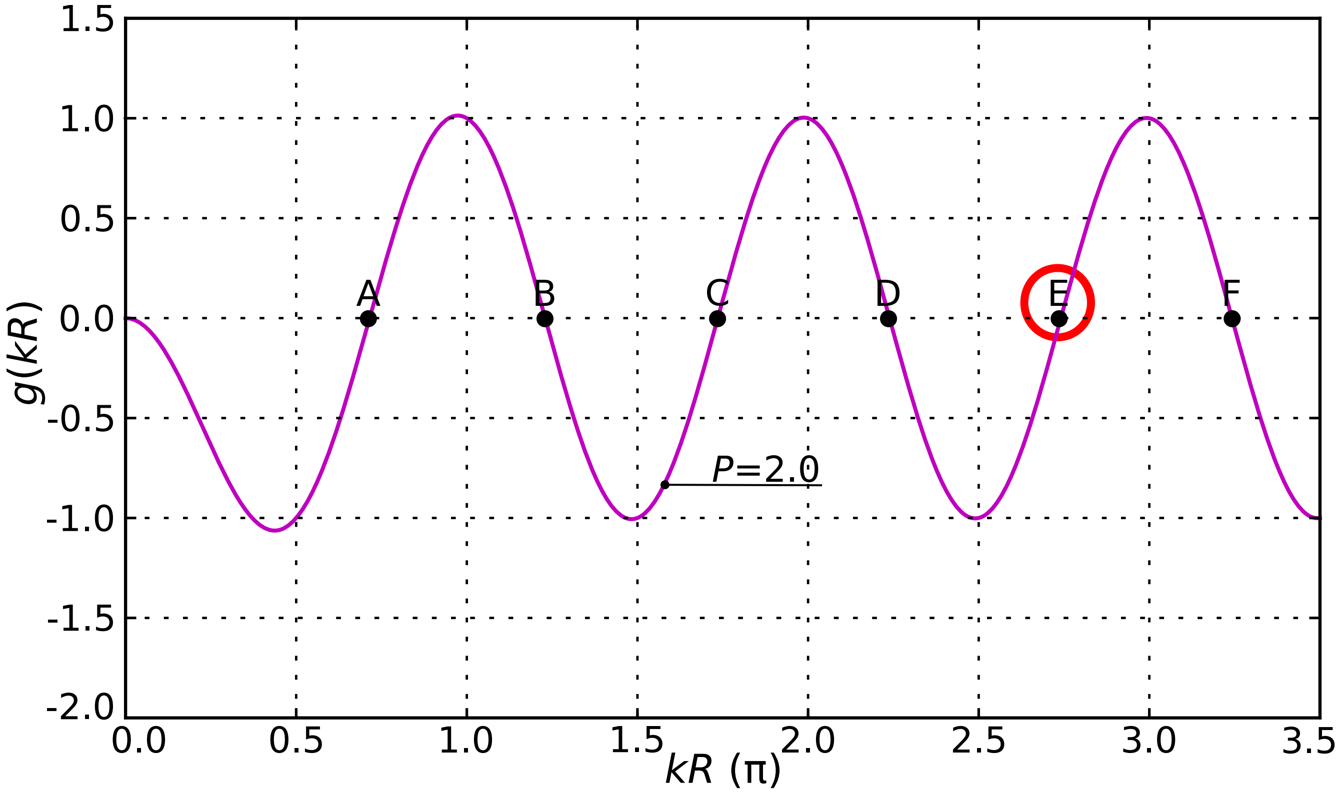

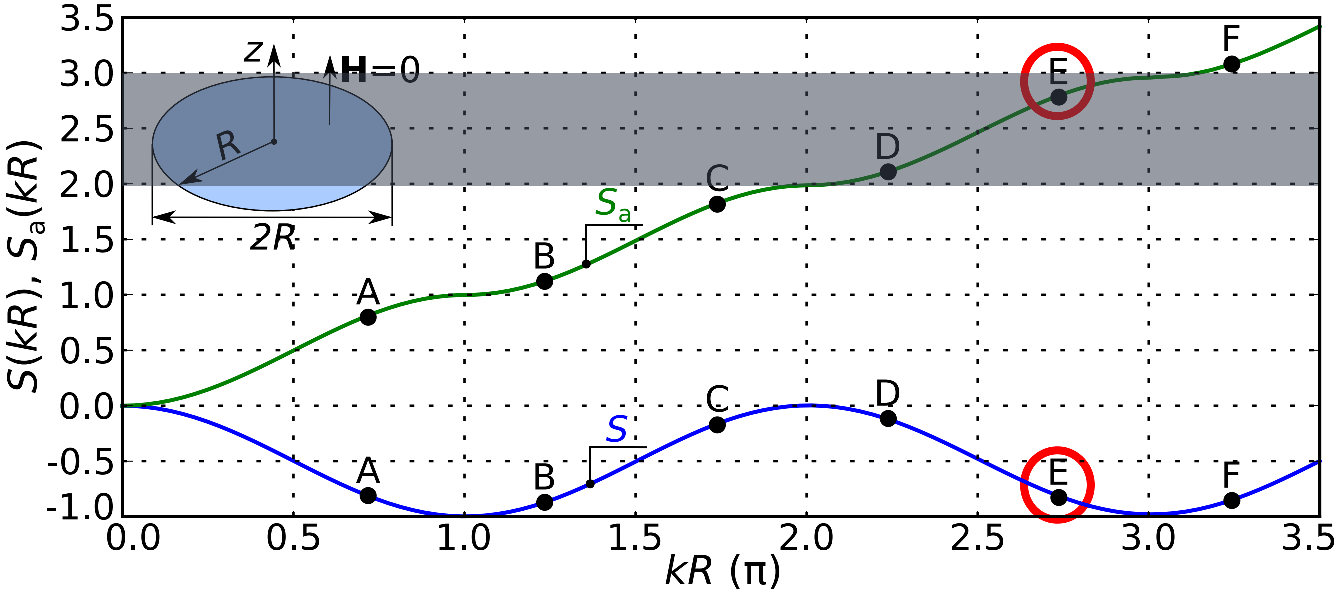

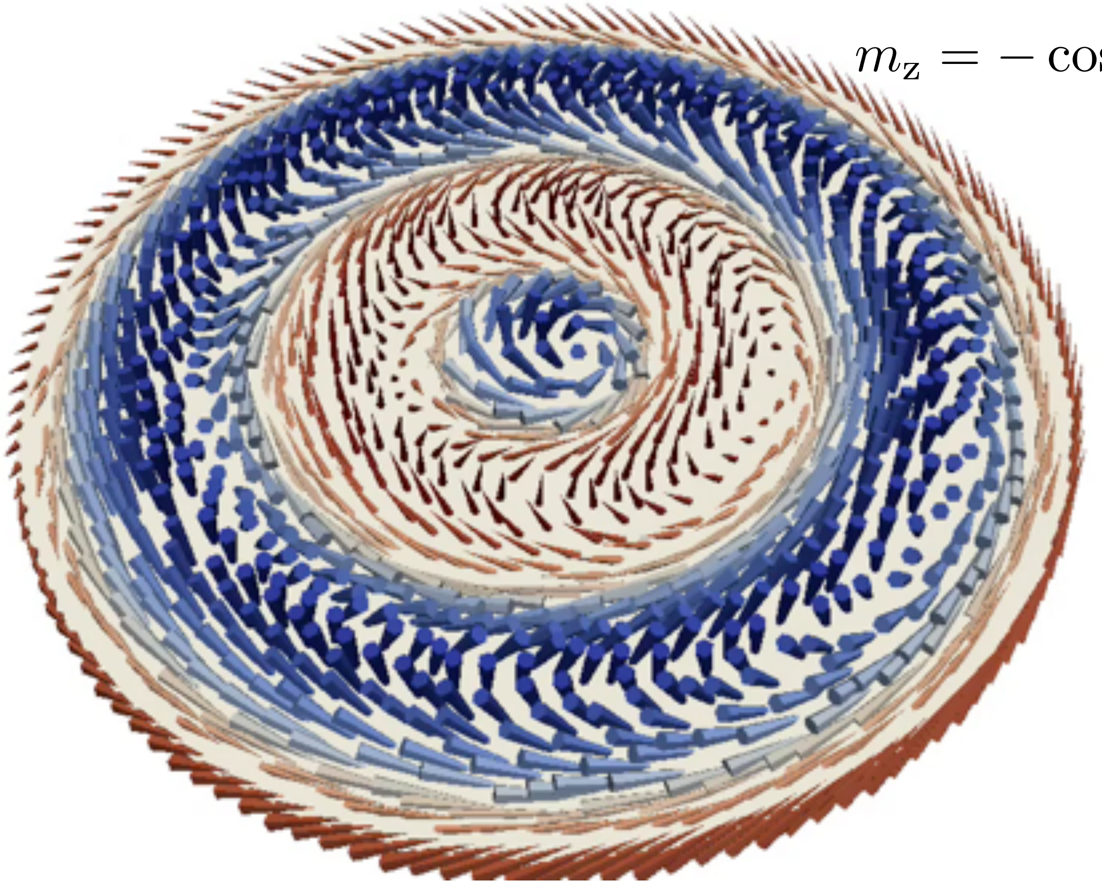

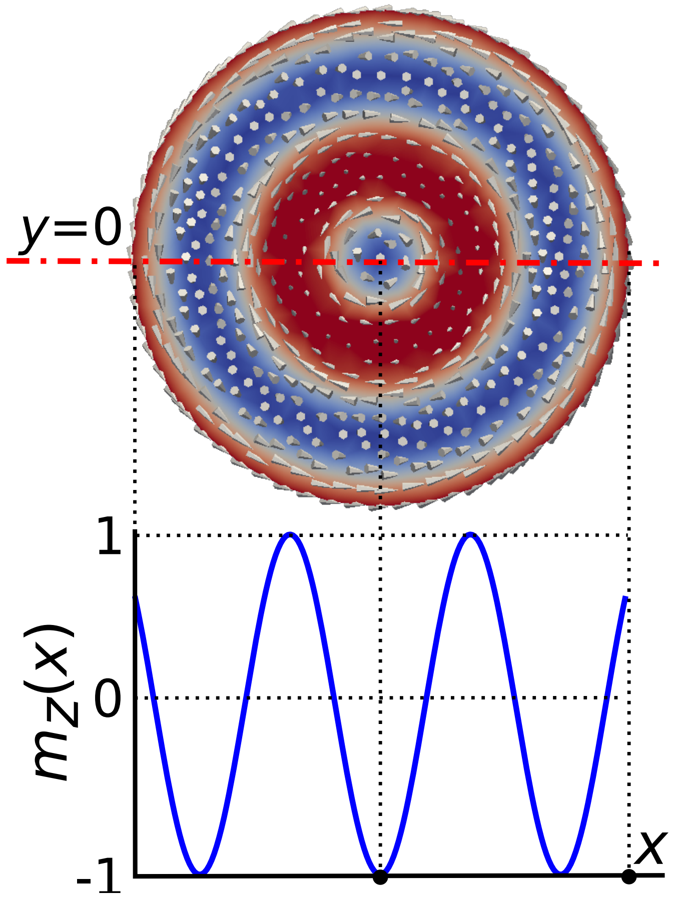

$$m_{\mathrm{r}} = 0$$

$$m_\theta = \sin(kr)$$

$$m_{\mathrm{z}} = -\cos(kr)$$

SOLUTION F

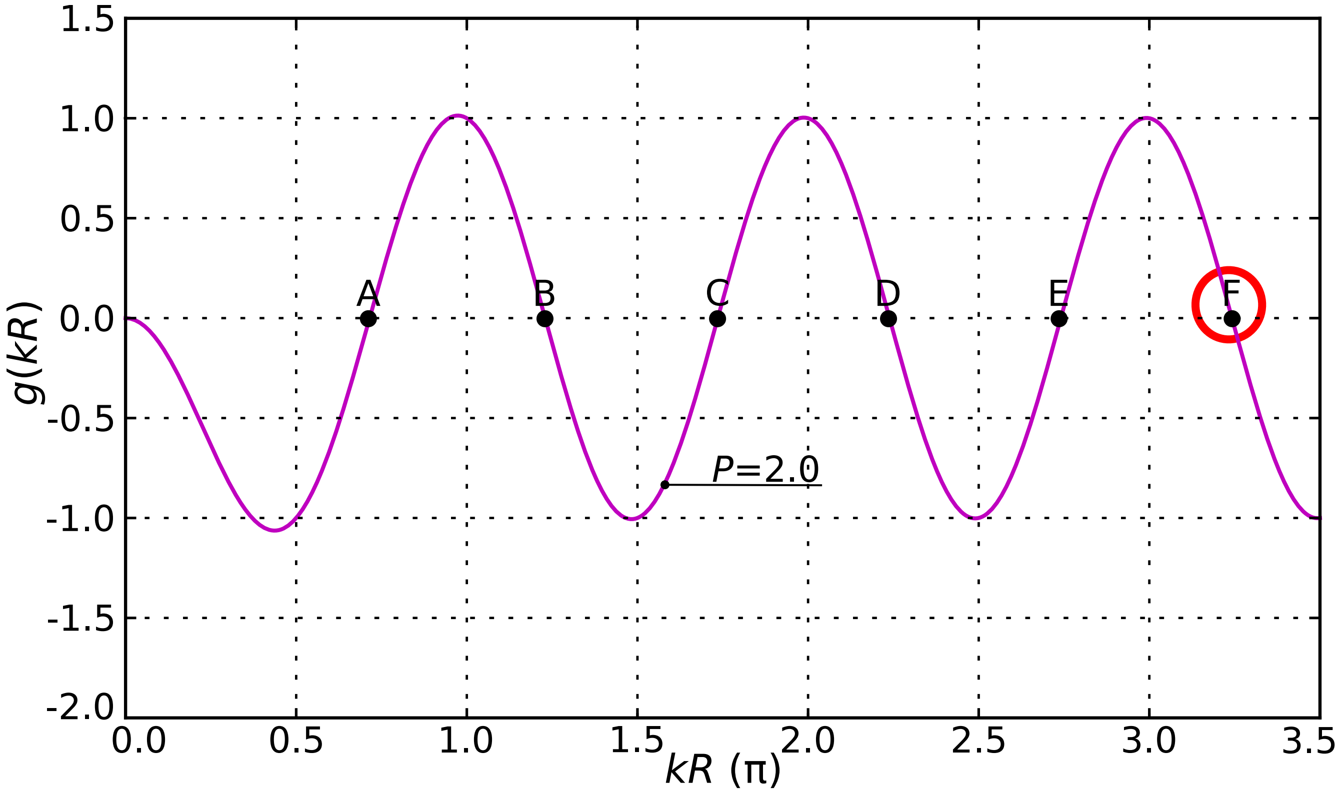

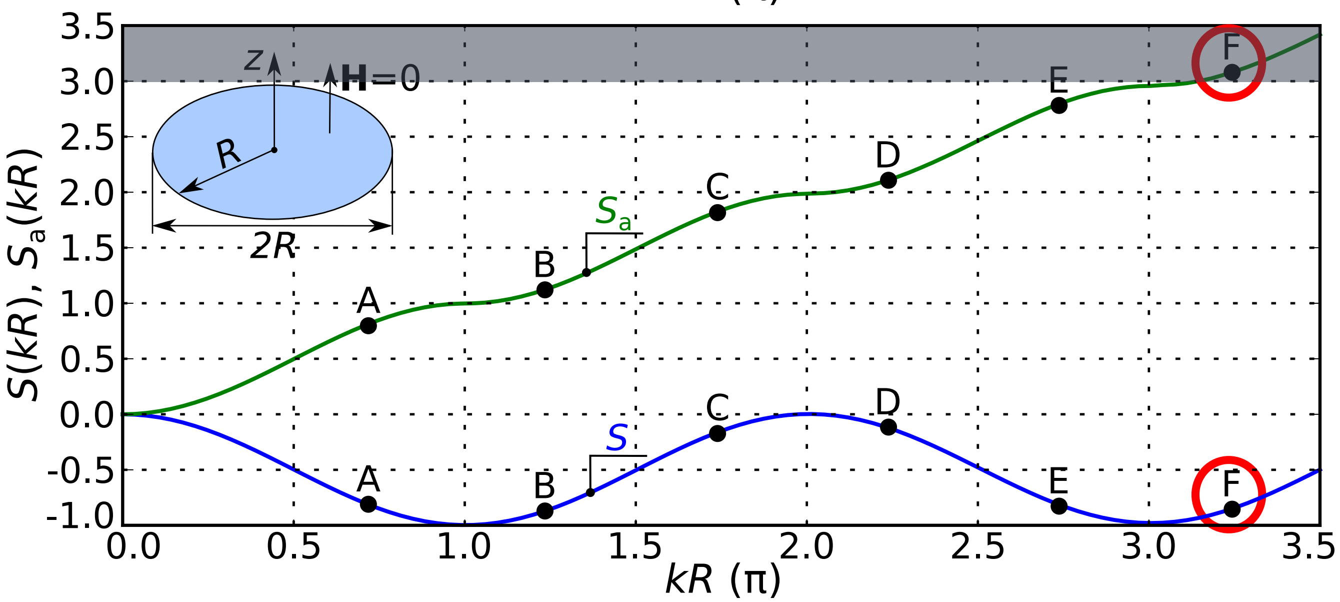

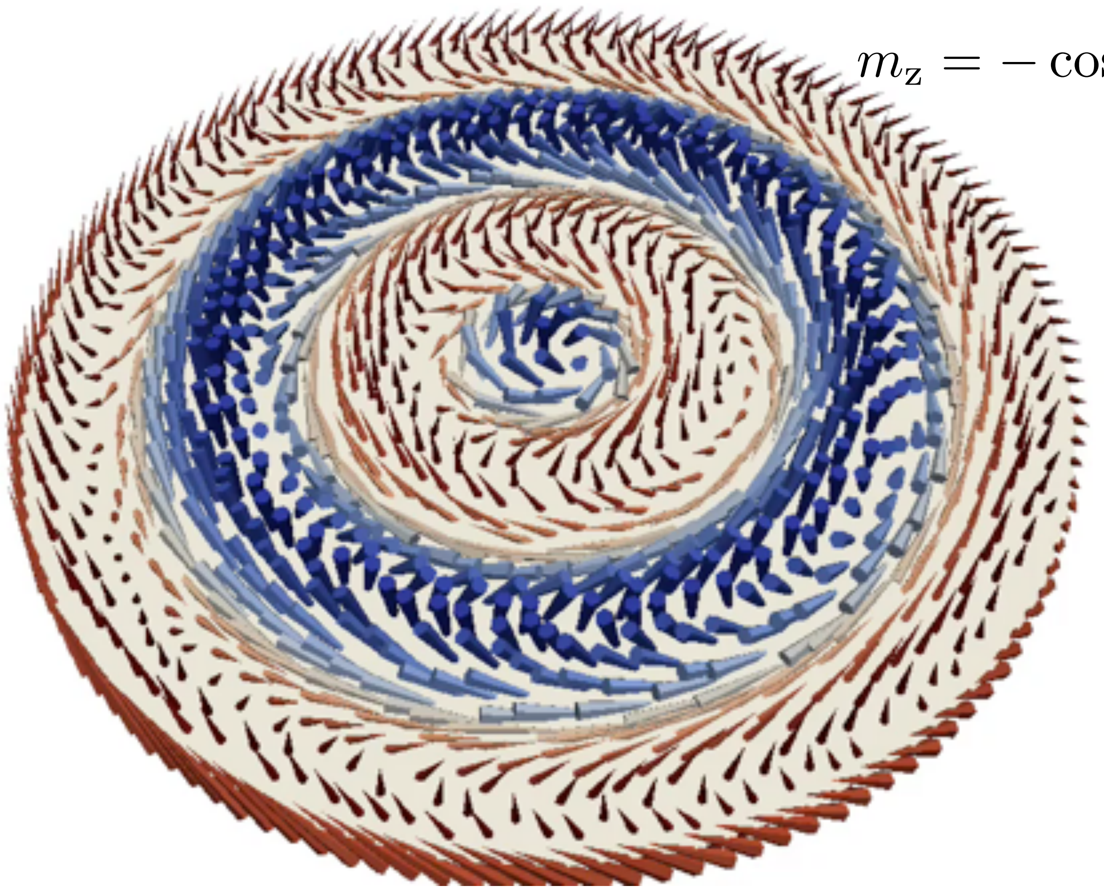

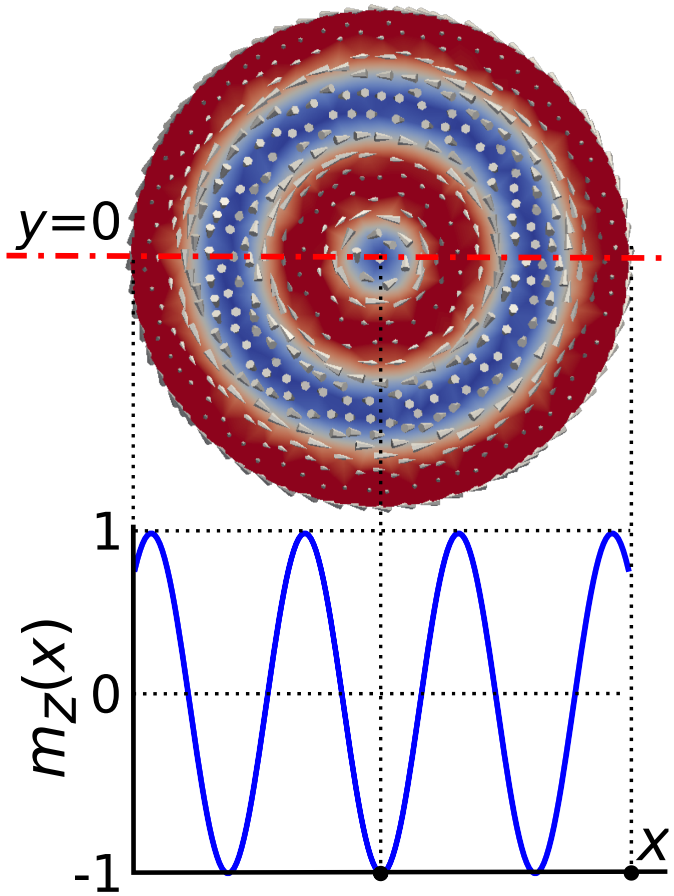

ANALYTIC MODEL RESULTS

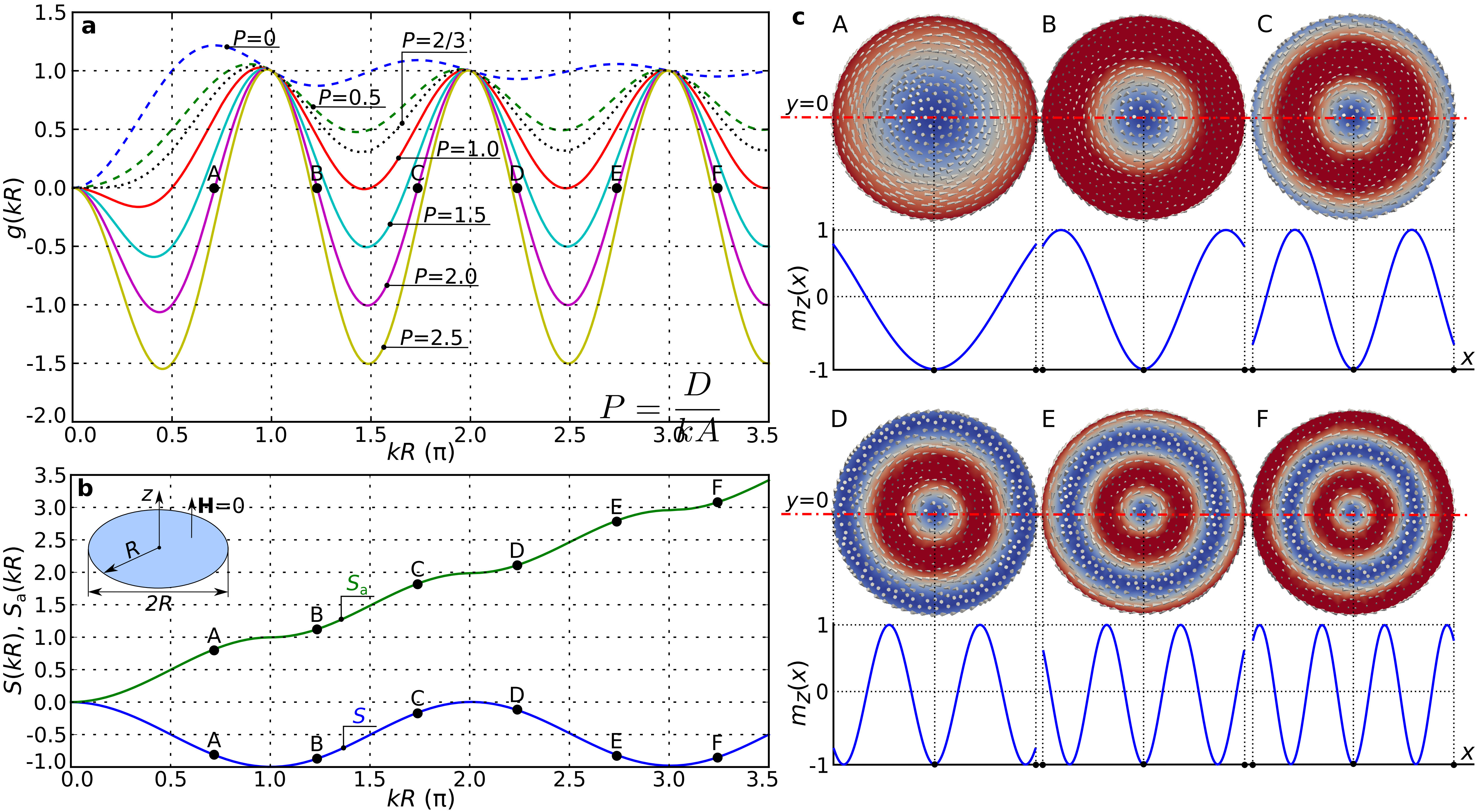

Du, H., Ning, W., Tian, M., & Zhang, Y. (2013), Physical Review B, 87, 014401.

Du, H., Ning, W., Tian, M., & Zhang, Y. (2013). EPL, 101(3), 37001.

SIMULATION RESULTS

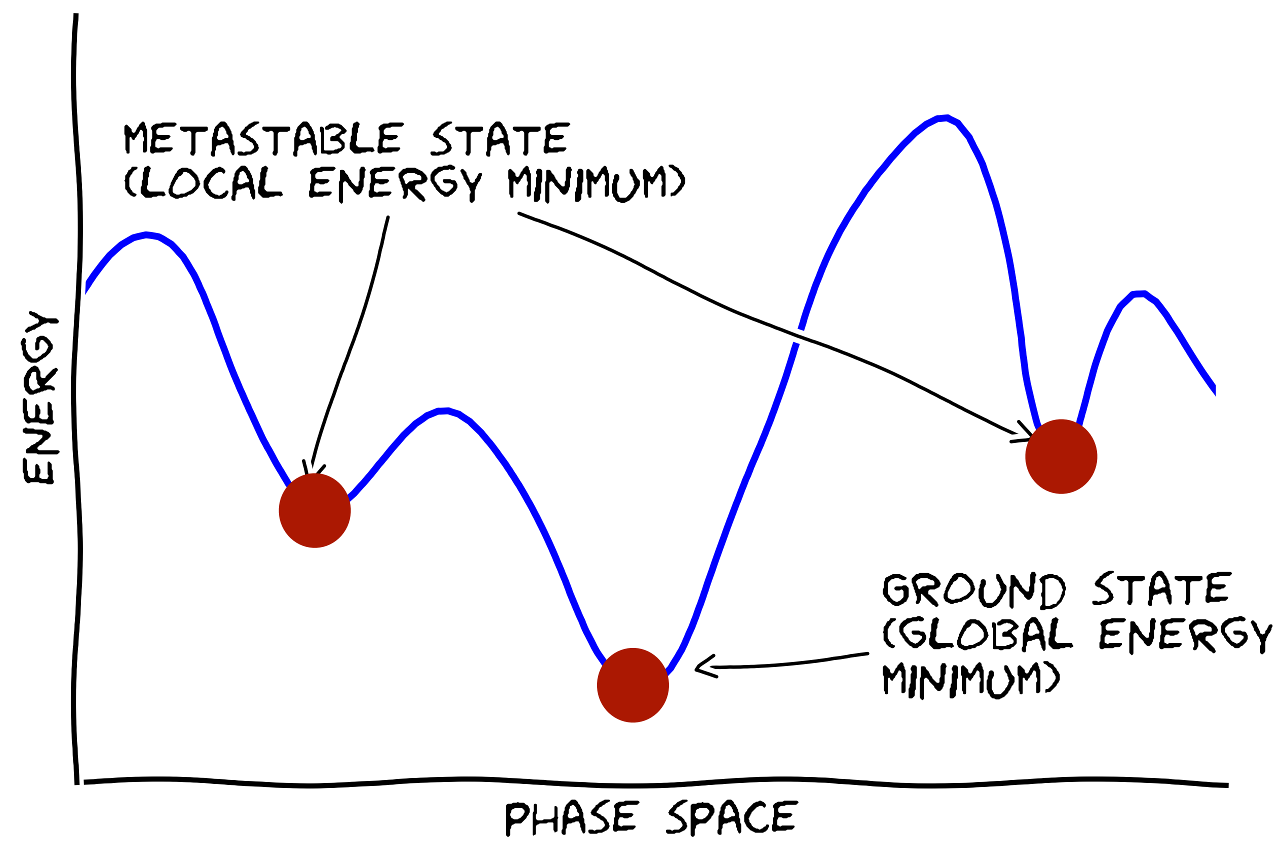

EQUILIBRIUM CONFIGURATIONS

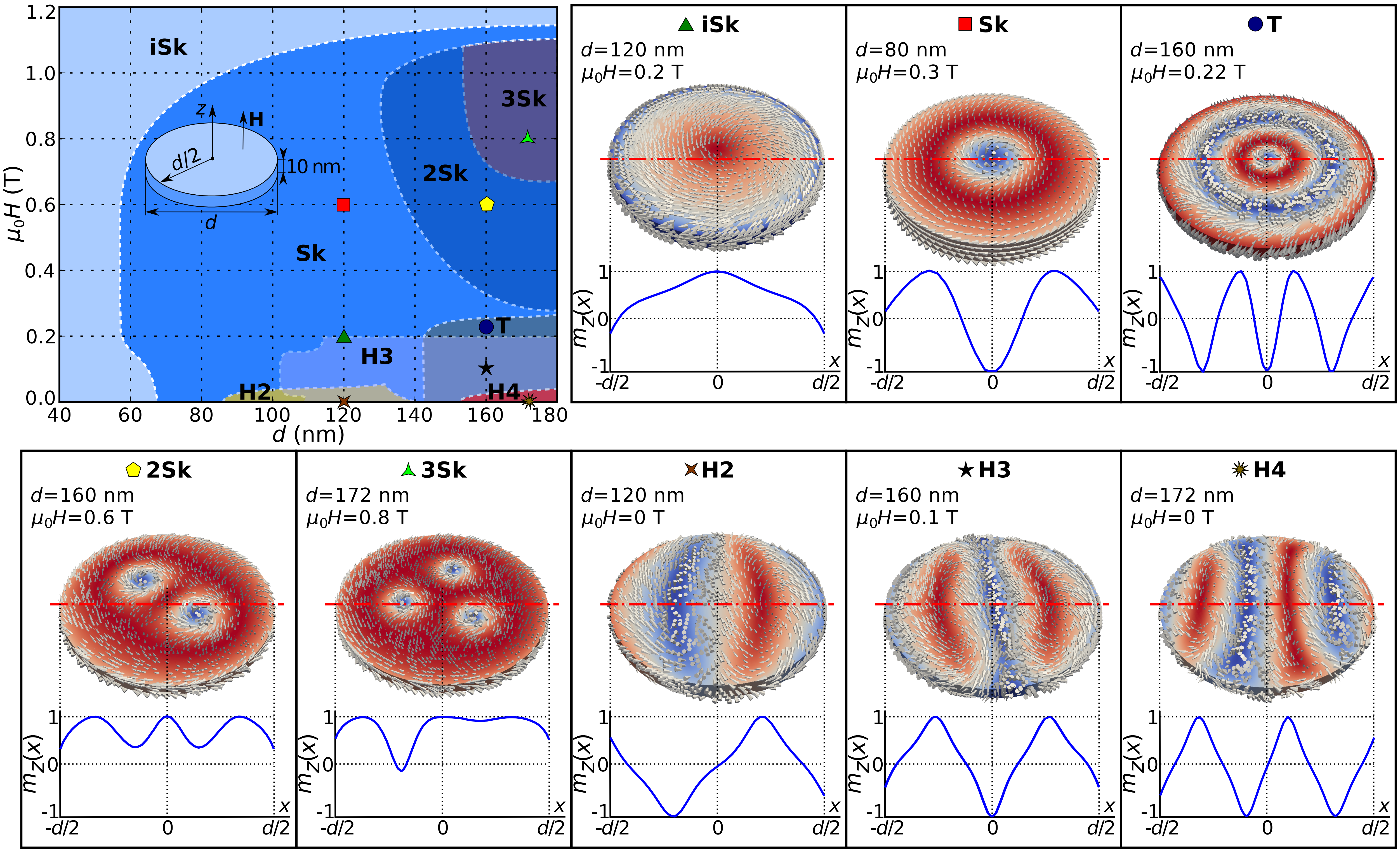

GROUND STATE PHASE DIAGRAM

- We select the state with the lowest energy
- **Two** different ground states.

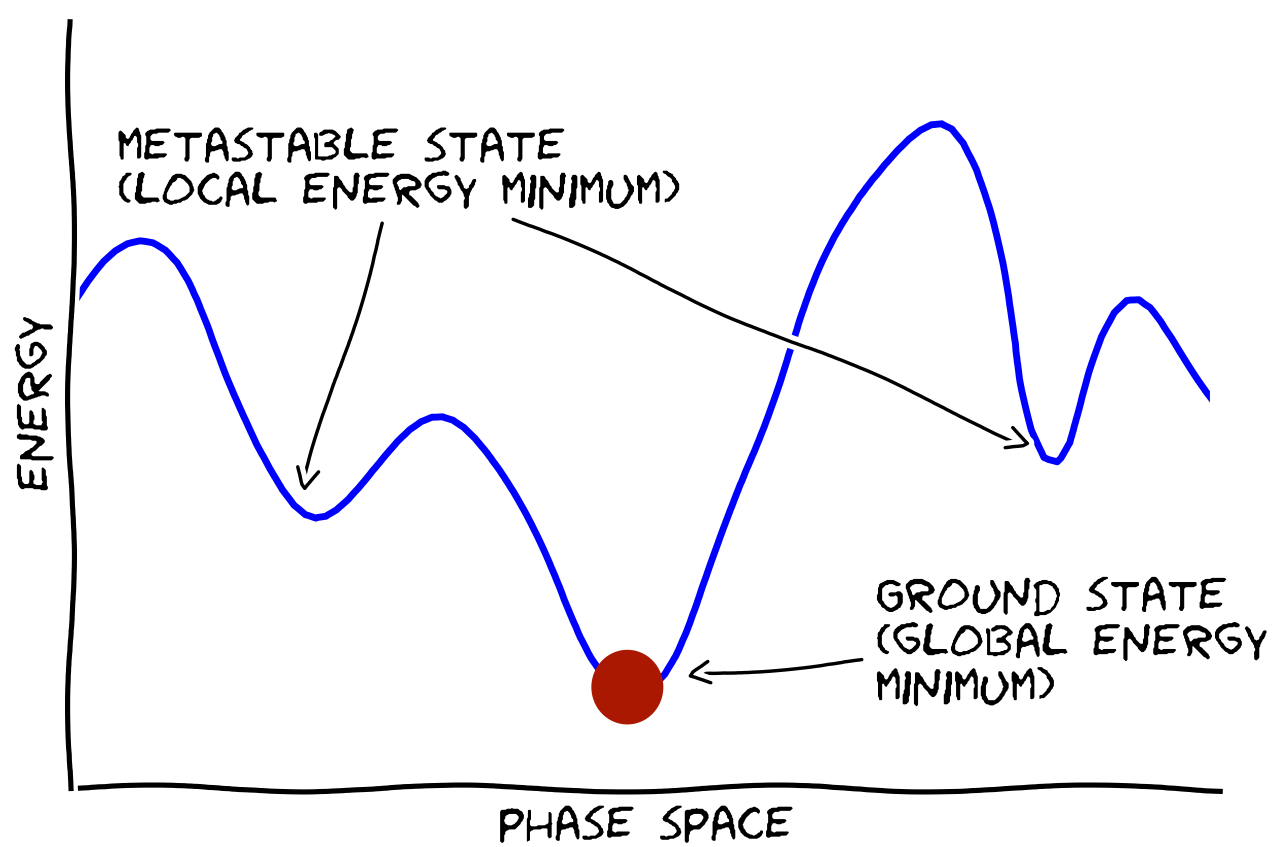

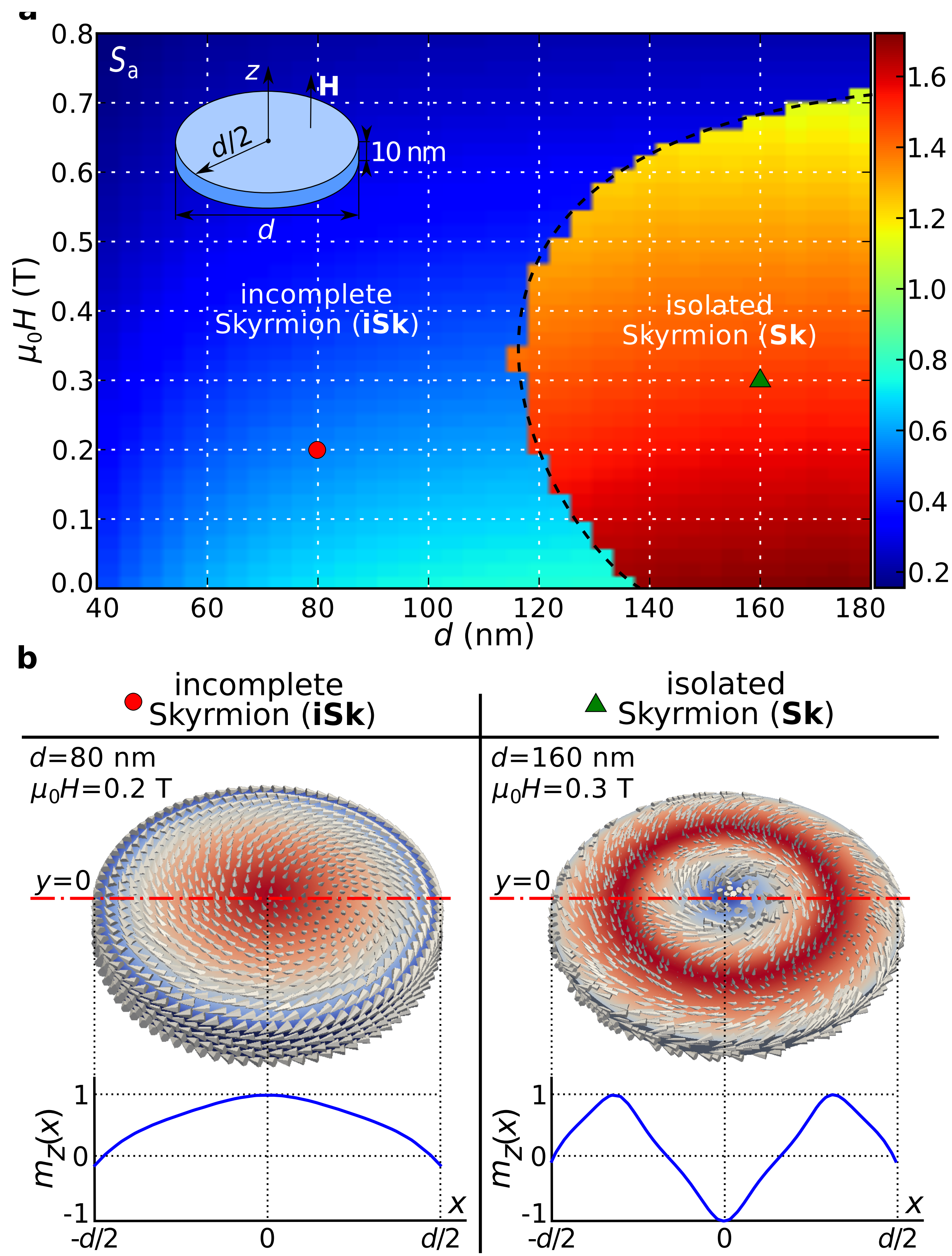

FeGe thin film disk phase diagram

INCOMPLETE SKYRMION (ISK)

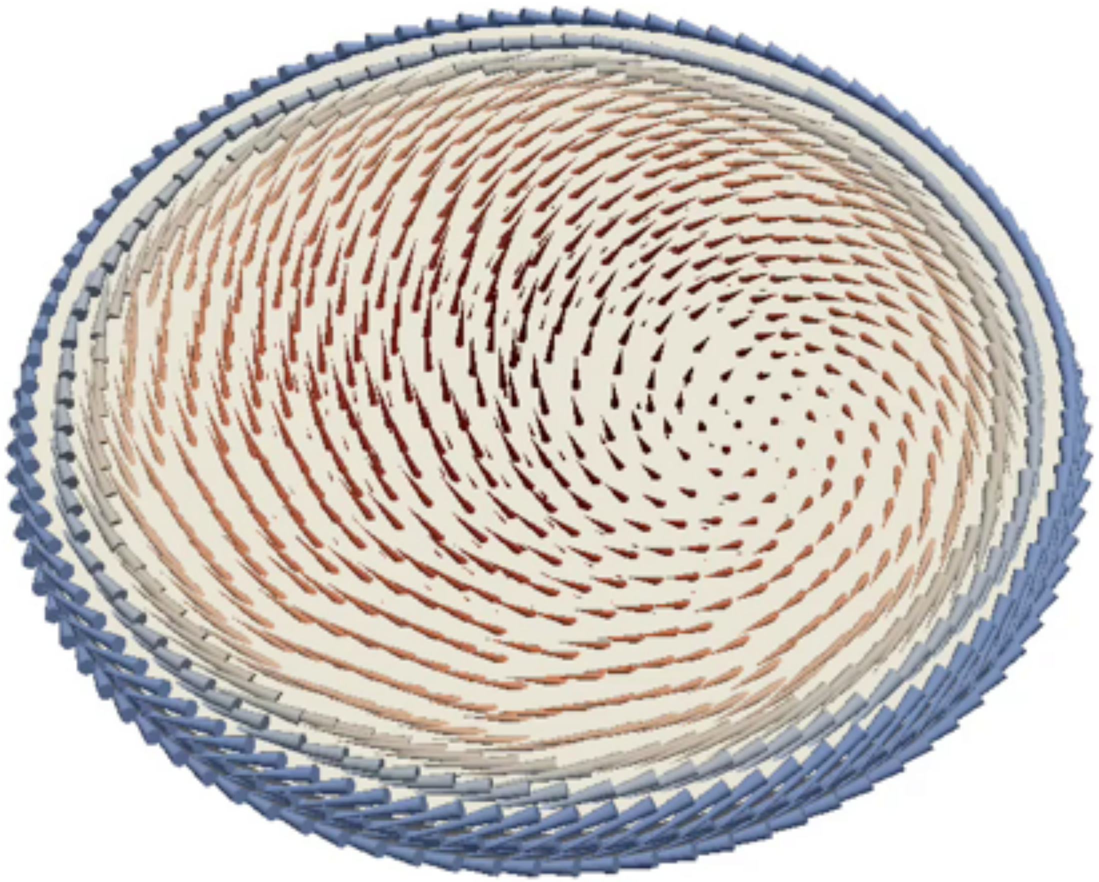

- No complete **spin rotation.**
- **|S| < 1**
- In literature also called **"quasi-ferromagnetic" or "vortex" state.**

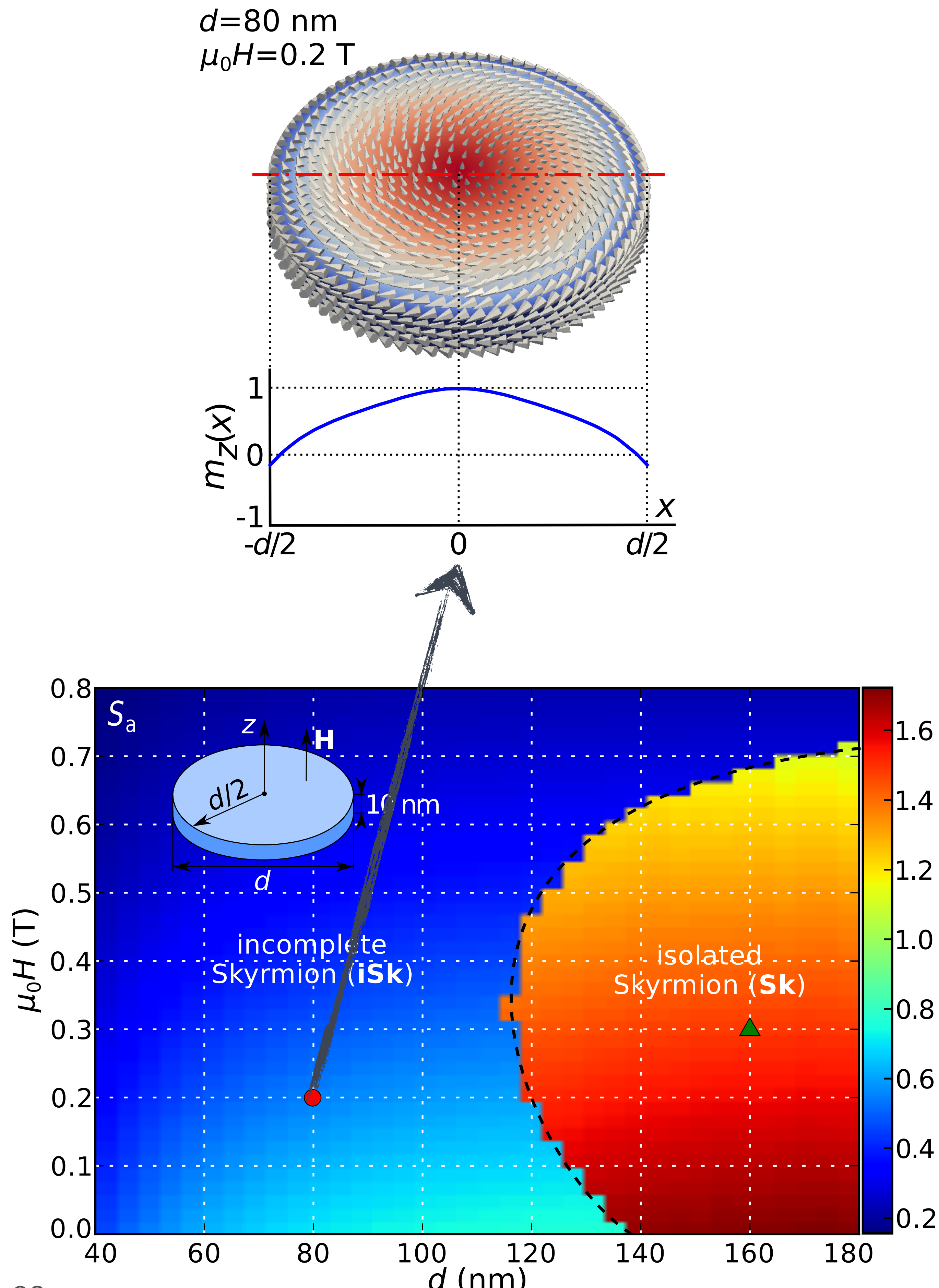

ISOLATED SKYRMION (SK)

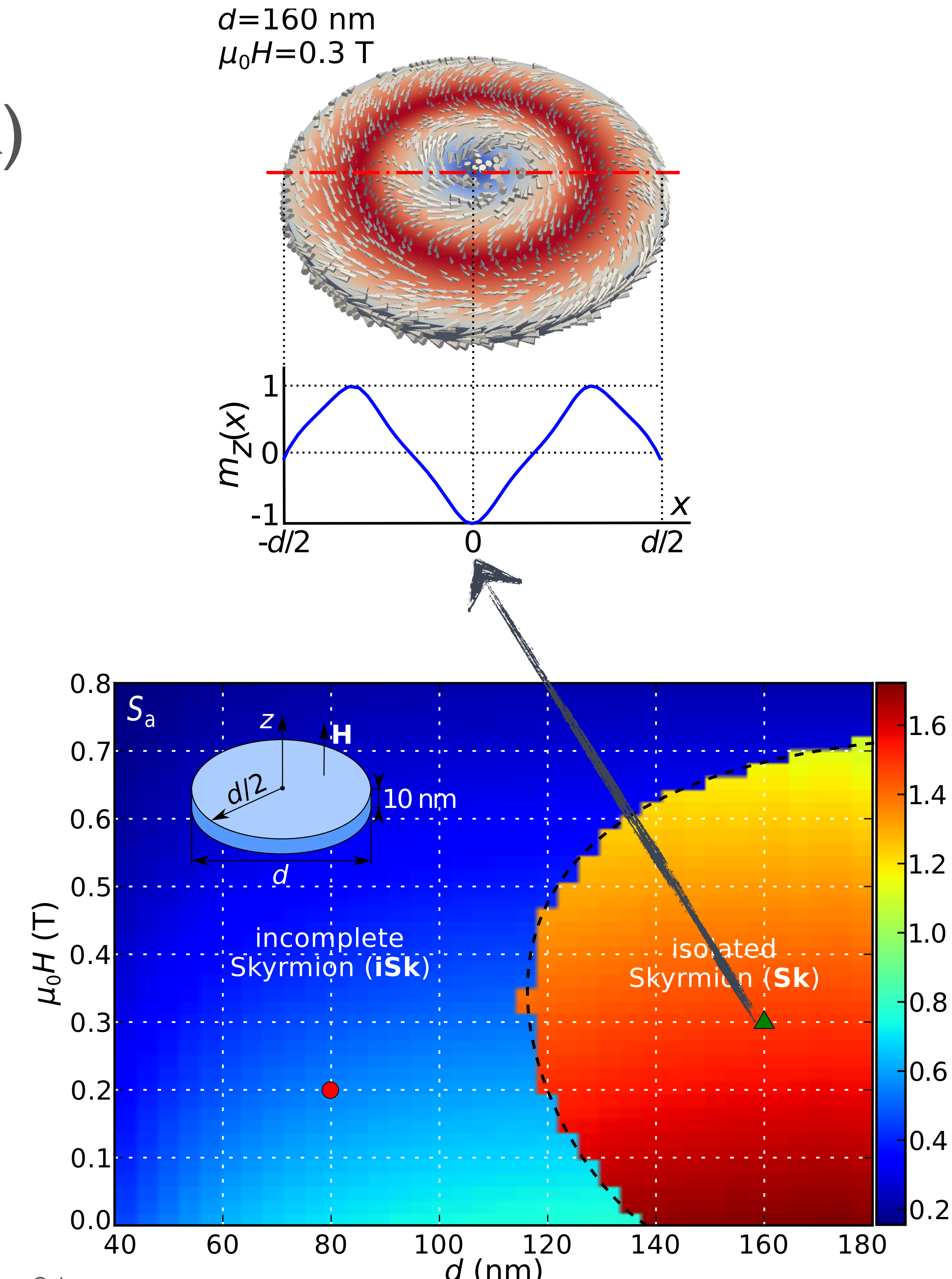

- Complete **spin rotation present.**
- **Significant tilt of magnetisation** at the edge which reduces |S|.

ENERGIES OF METASTABLE STATES

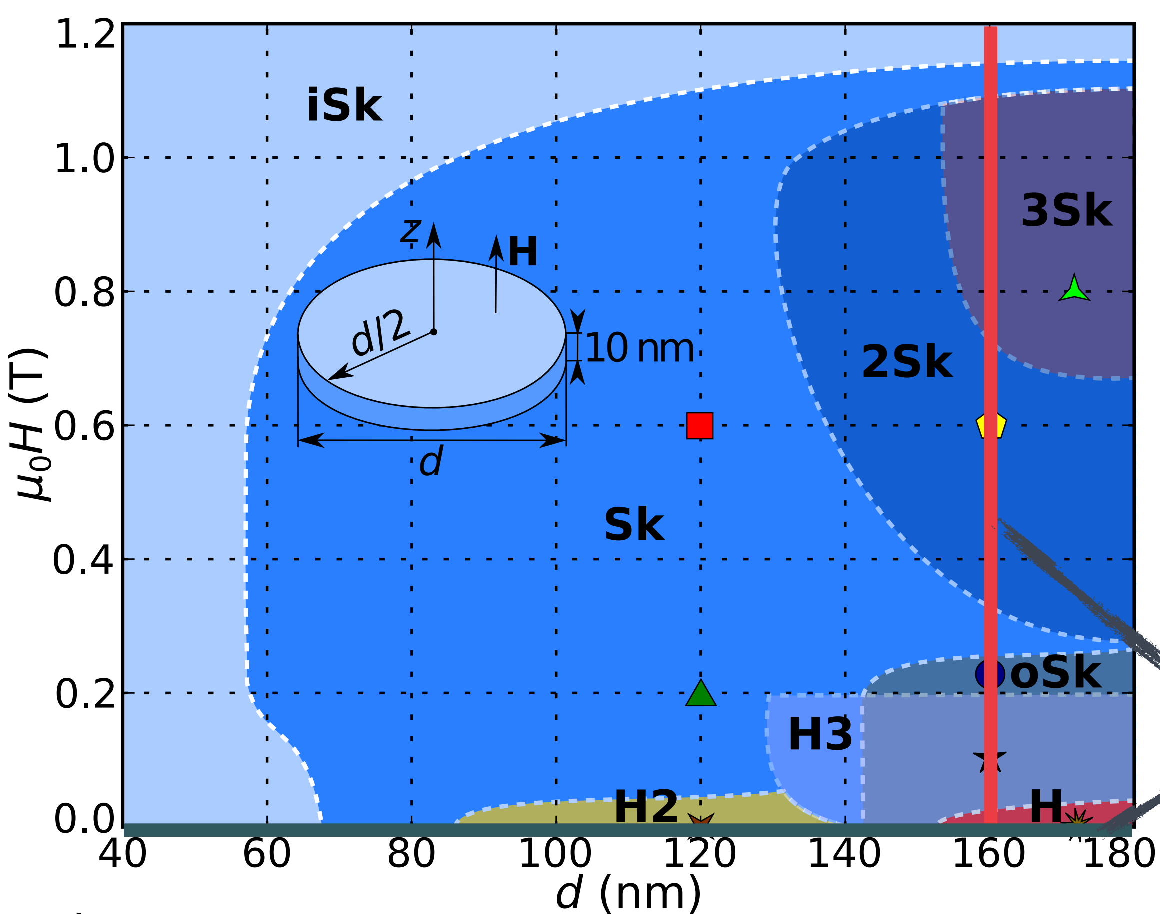

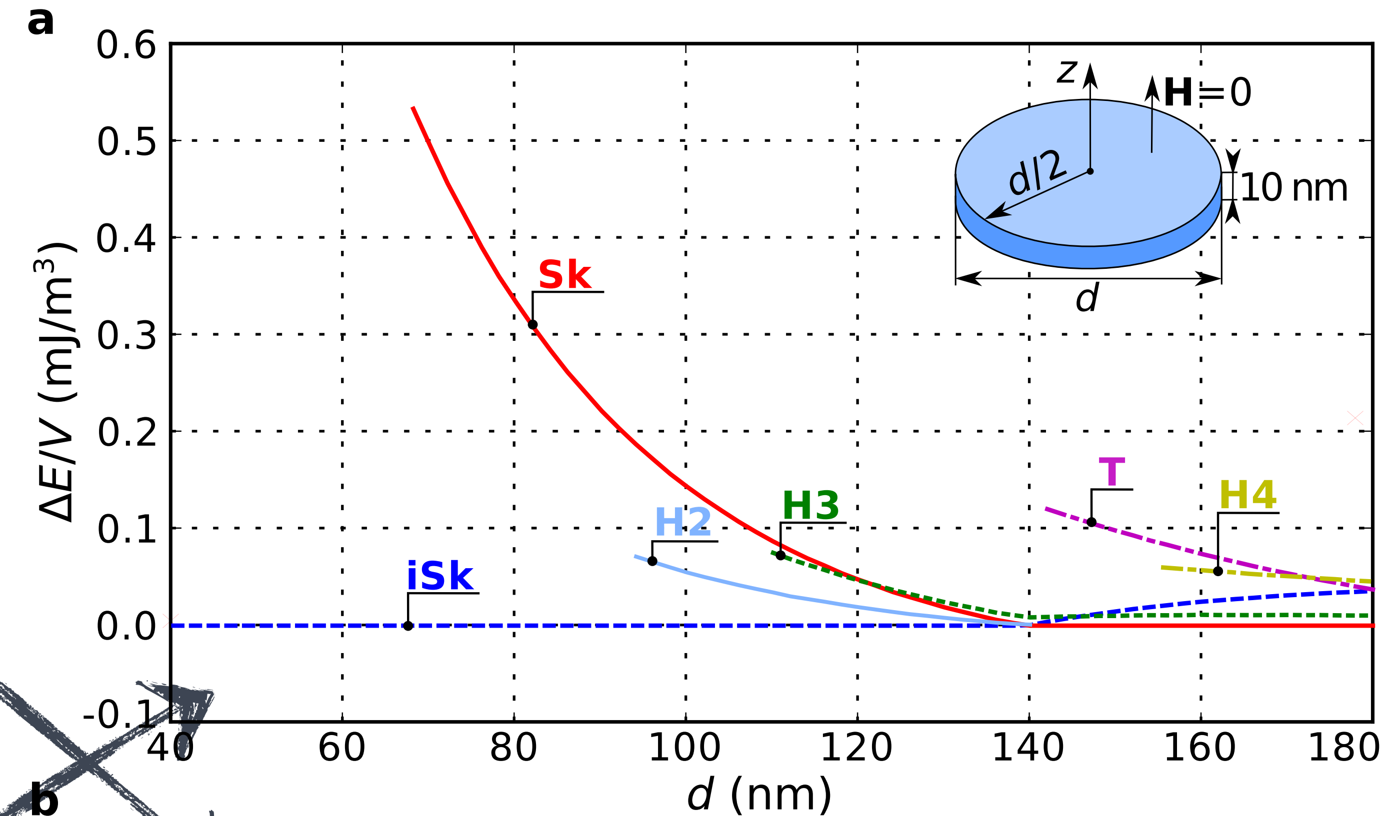

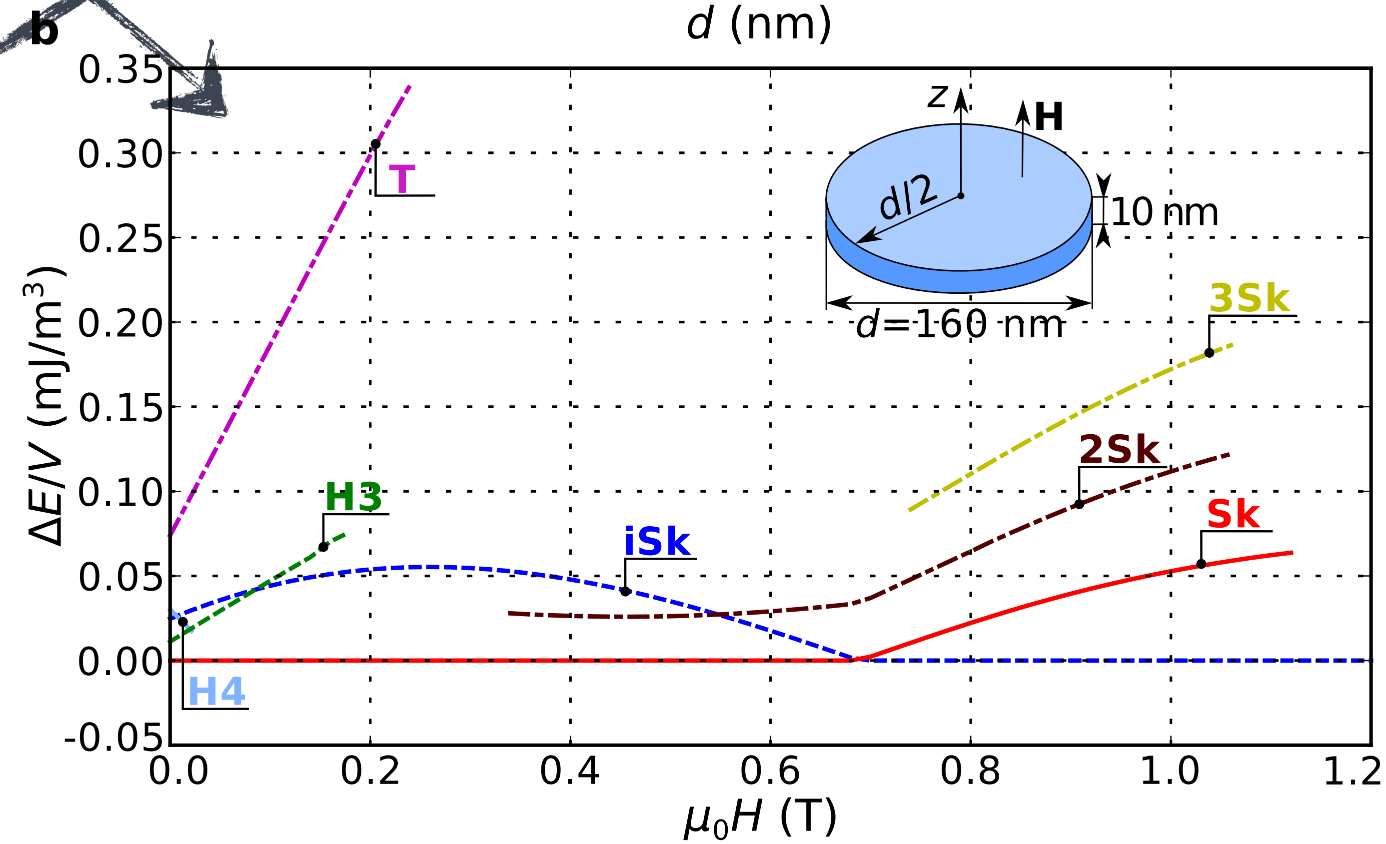

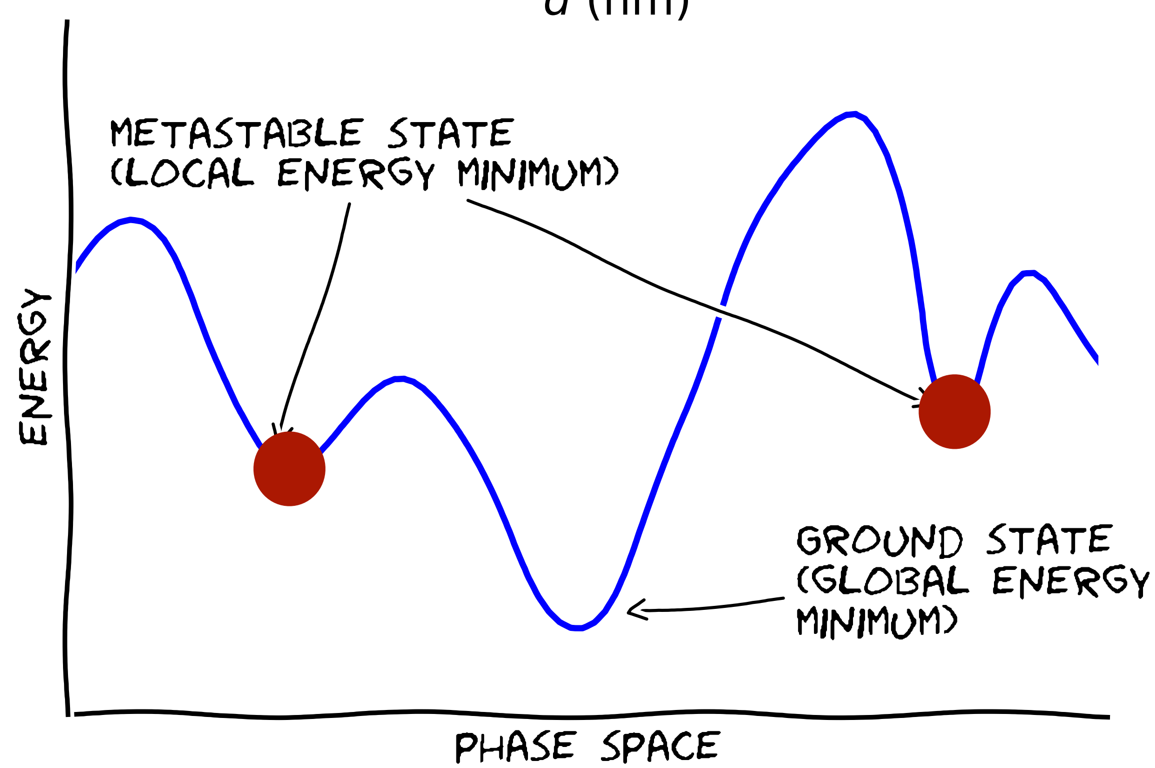

ROBUSTNESS

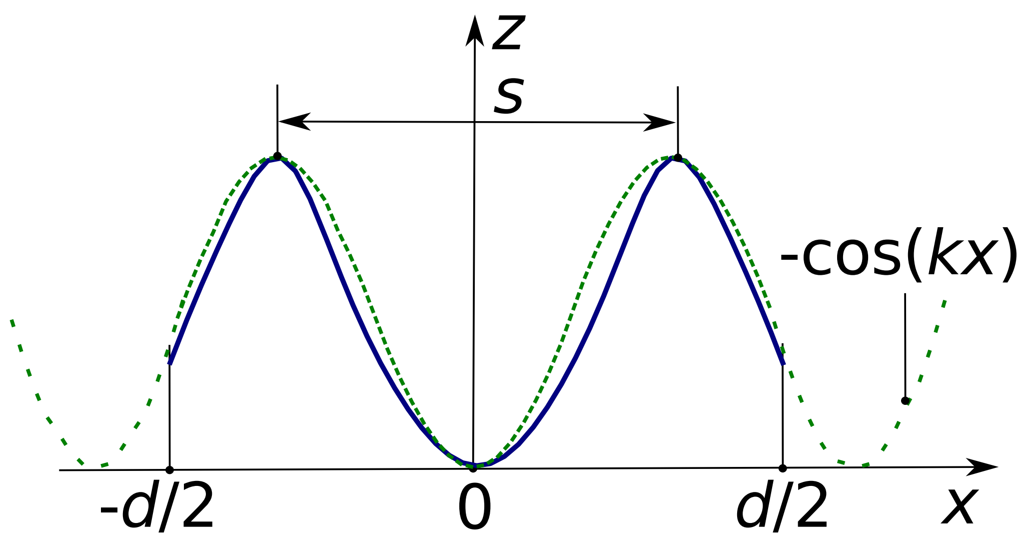

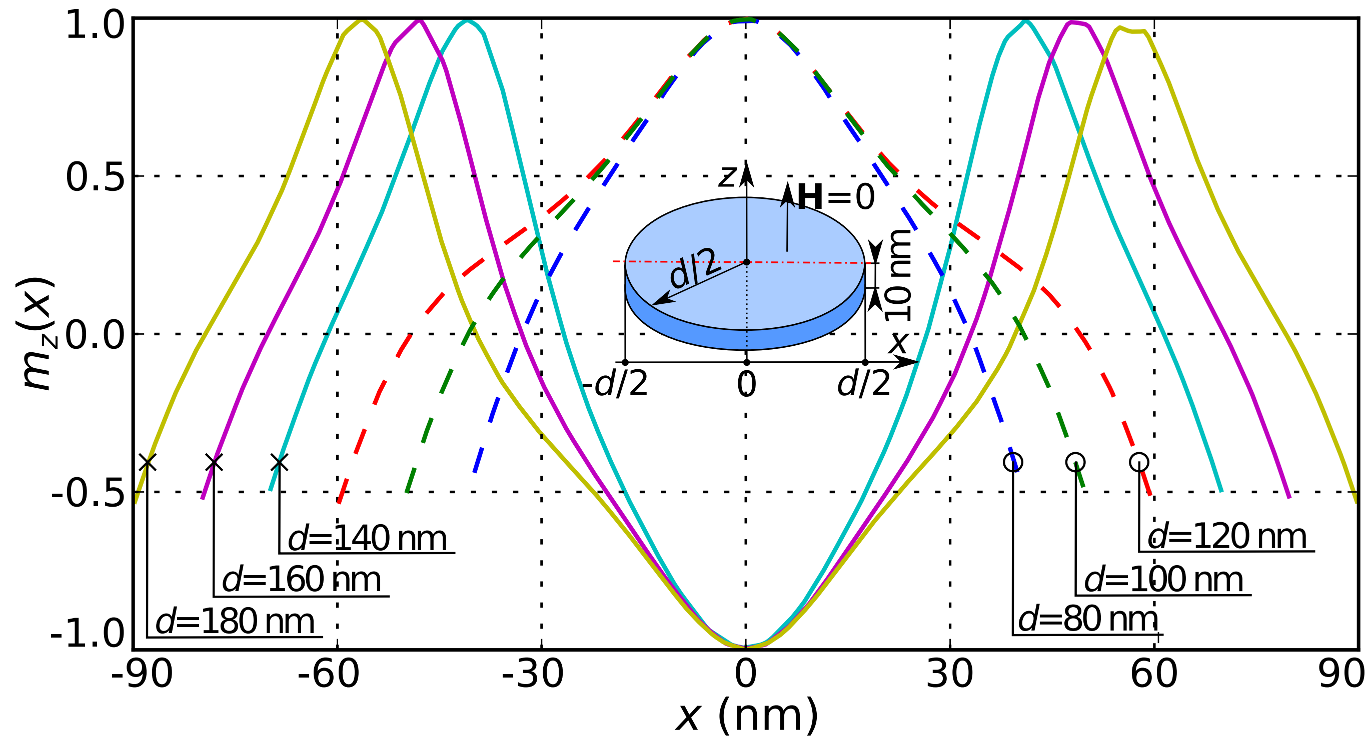

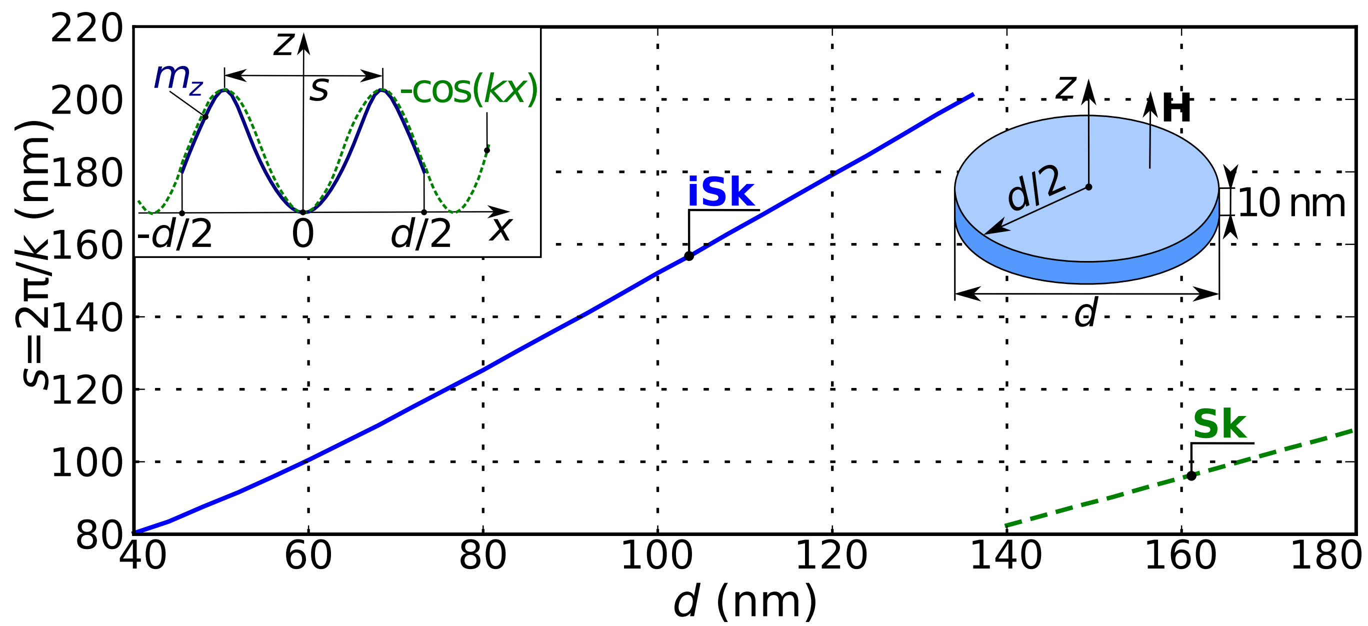

- Skyrmionic textures **able to adapt their size** to accommodate the size of a hosting nanostructure.
- This provides the **robustness** of technology built on skyrmions.
- iSk and Sk have **different core orientation**.

POSSIBLE STABILISING MECHANISM

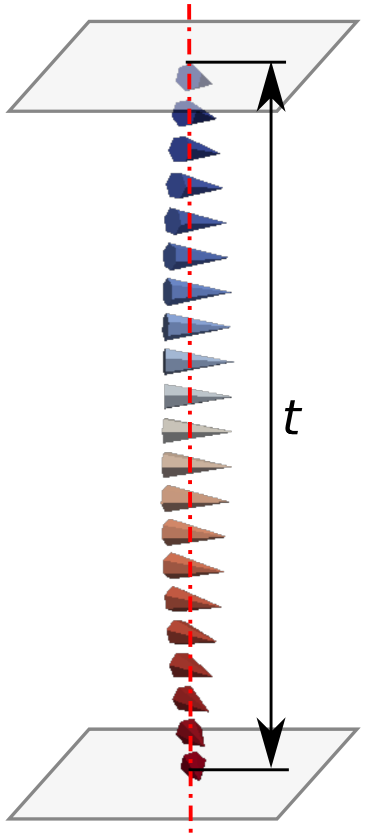

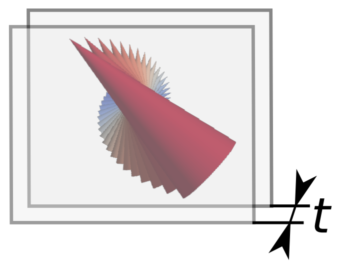

Rybakov *et al.*, PRB **87**, 094424 (2013)

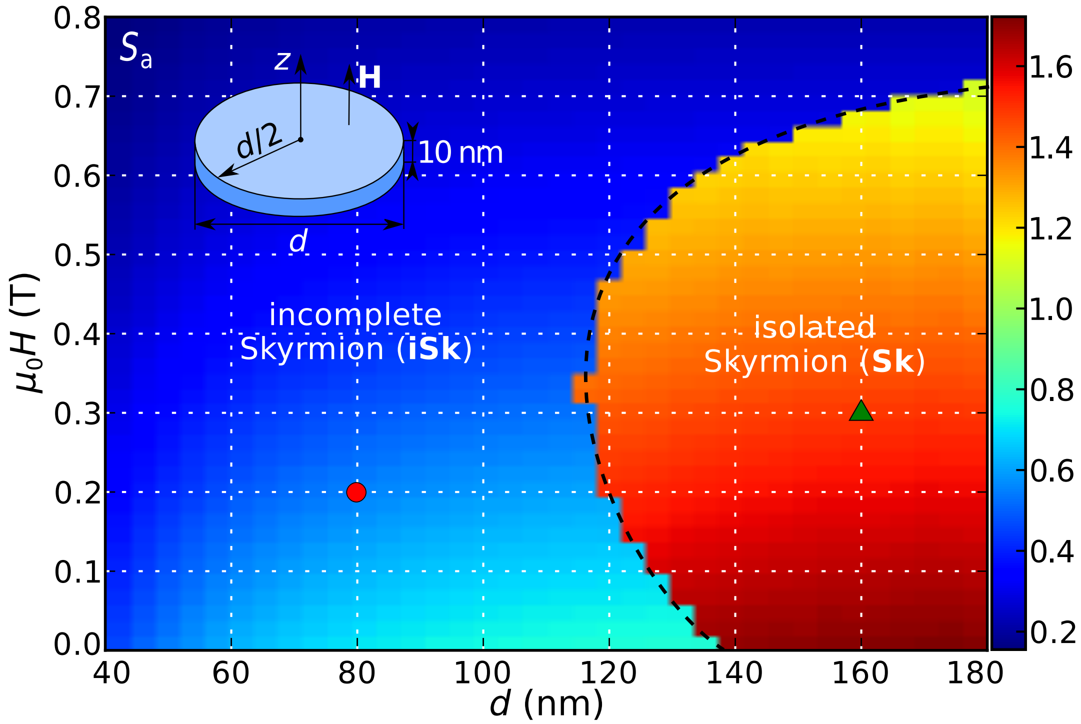

no demagnetisation

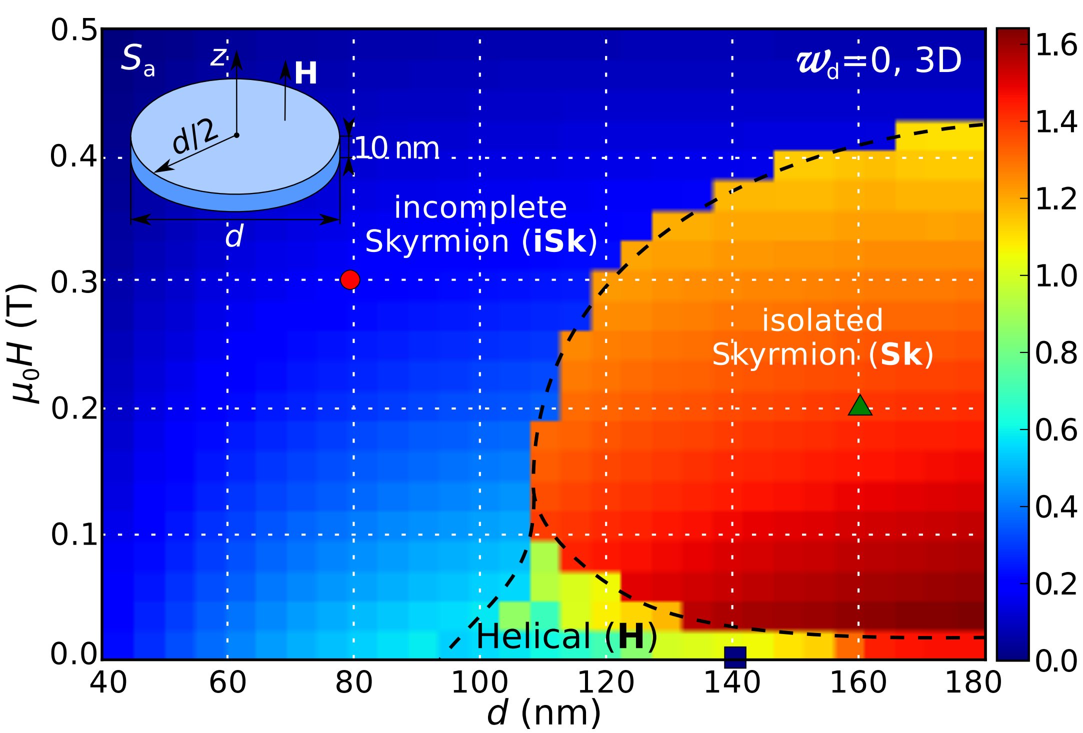

2D

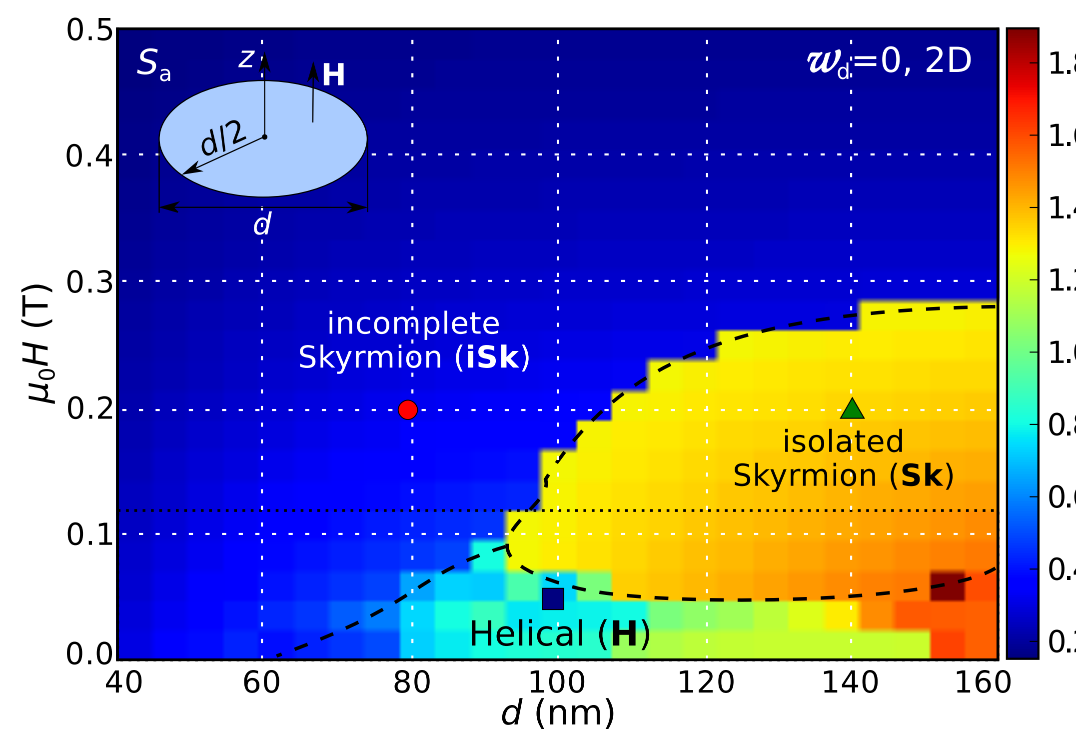

POSSIBLE STABILISING MECHANISM

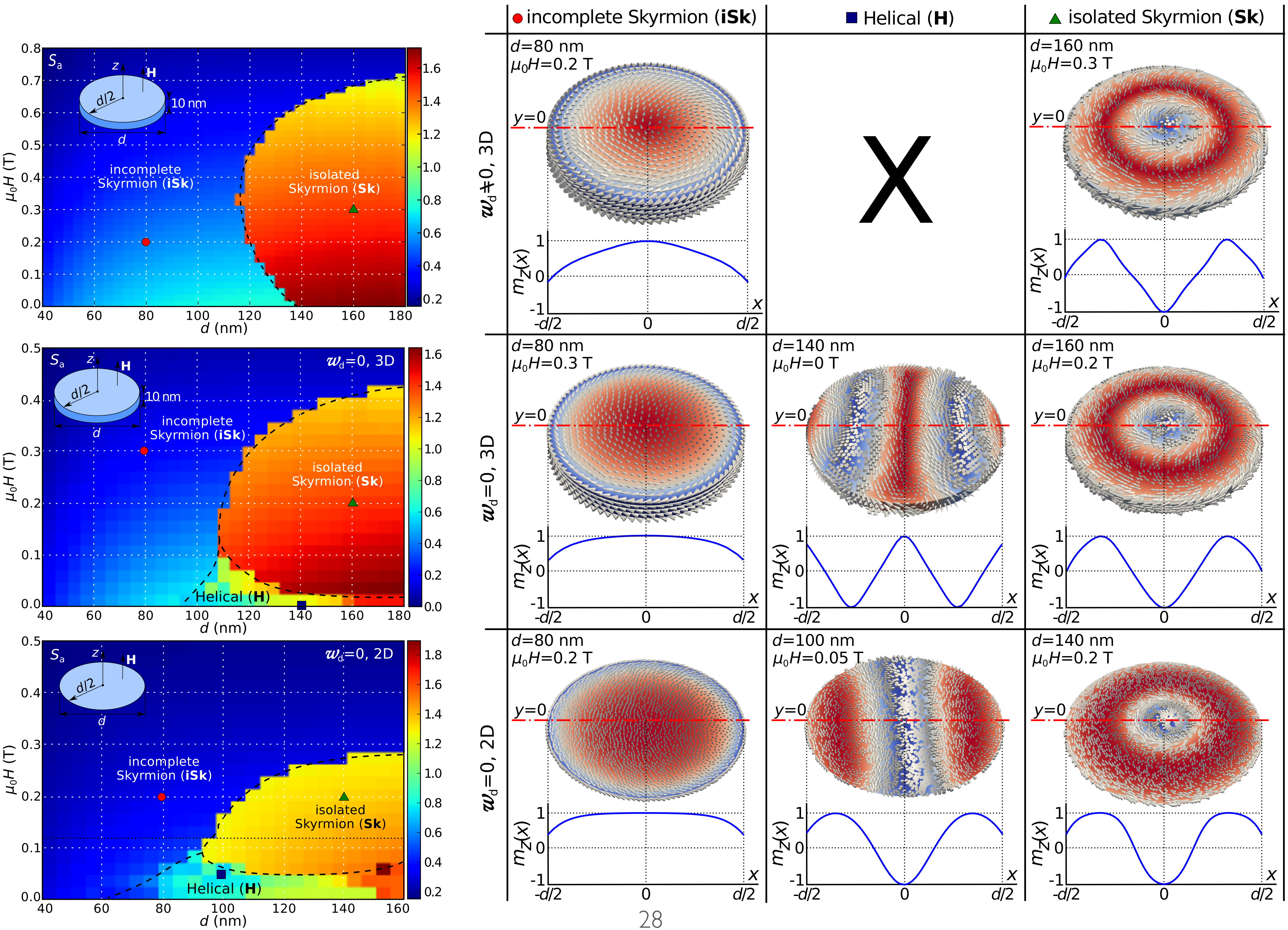

HYSTERETIC BEHAVIOUR

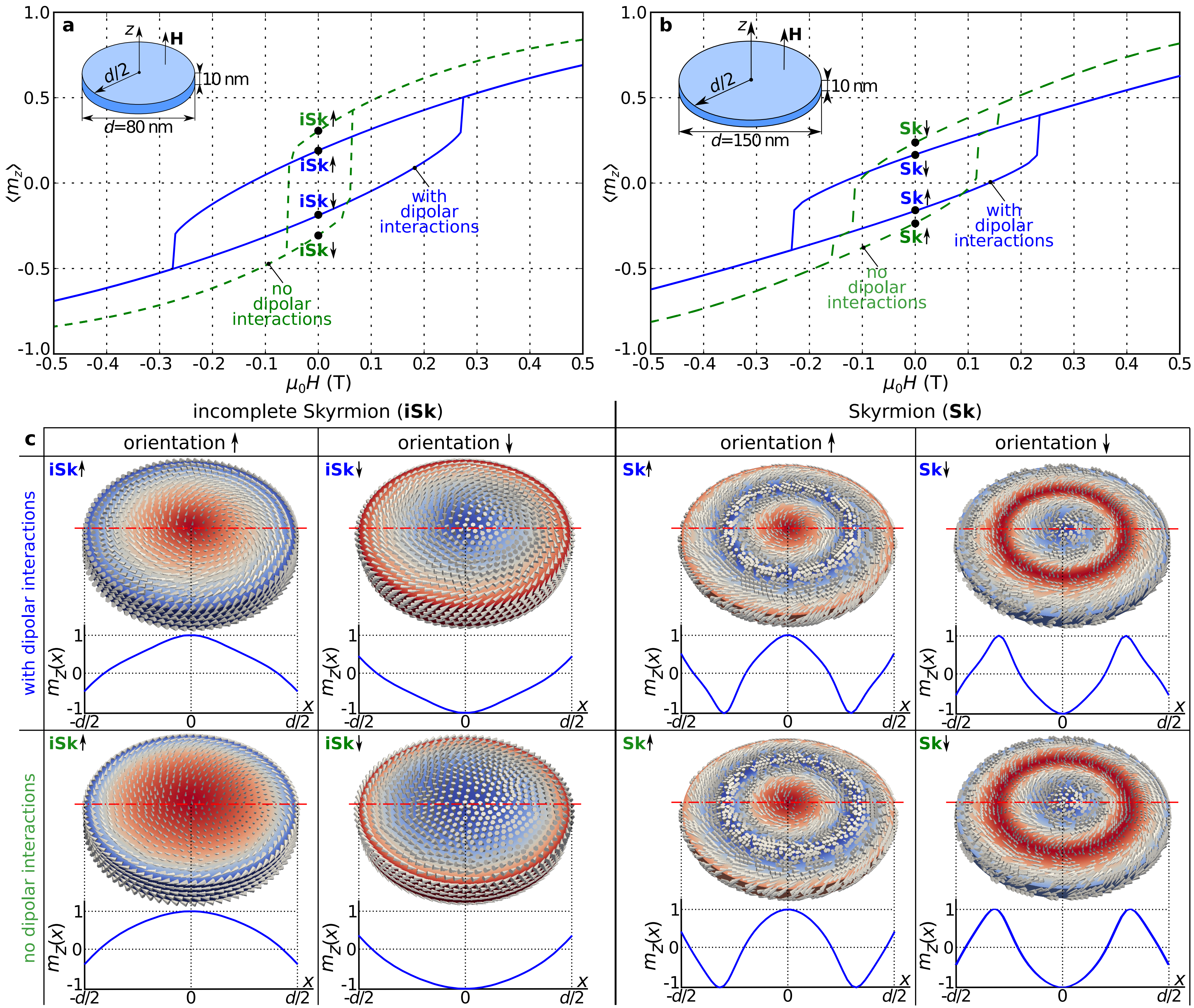

HYSTERETIC BEHAVIOUR (ISK)

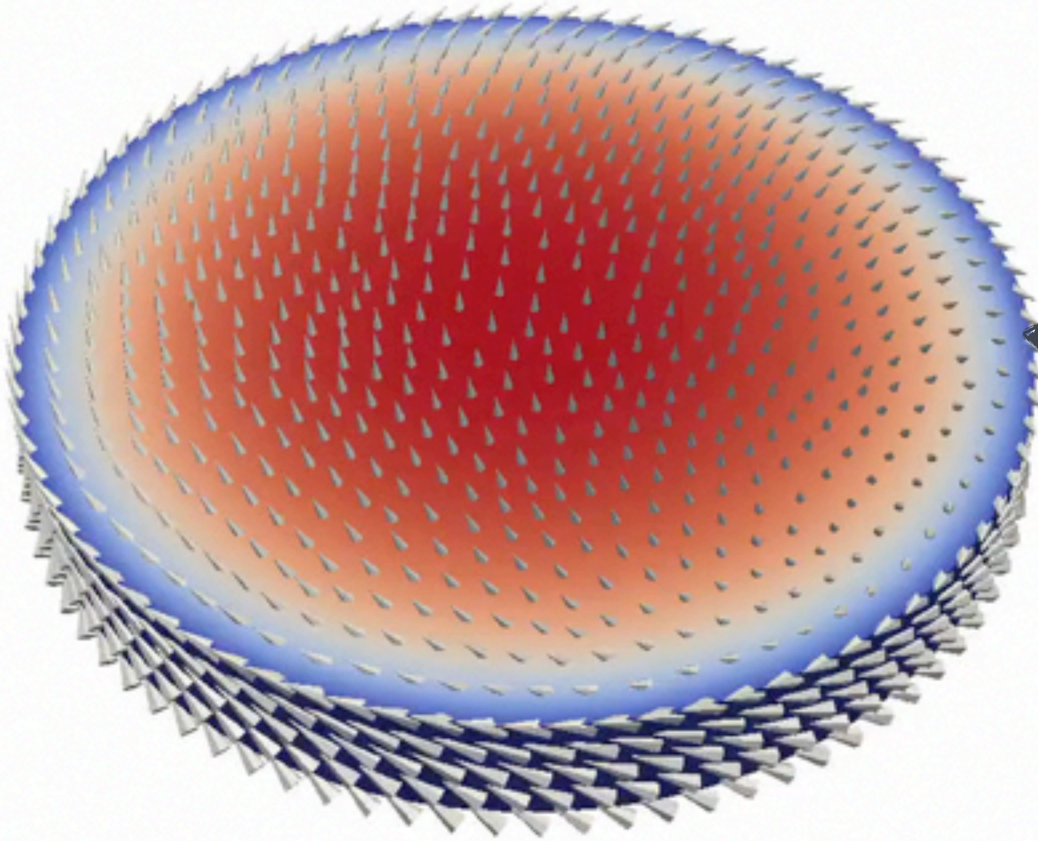

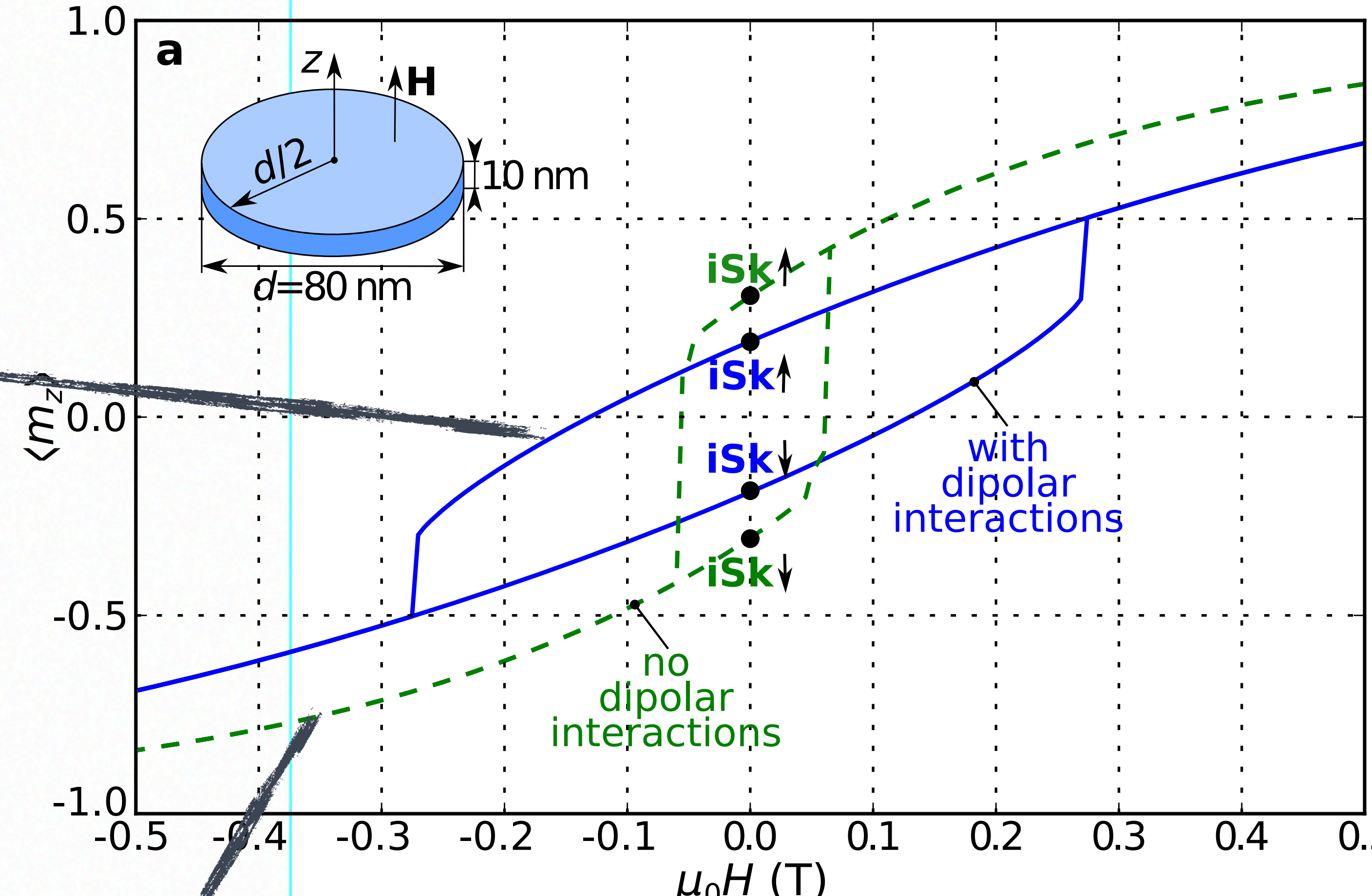

Hysteretic behaviour remains **in absence of** magnetocrysralline anisotropy and dipolar-based shape anisotropy, suggesting the existence of Dzyaloshinskii-Moriya based shape anisotropy.

HYSTERETIC BEHAVIOUR (SK)

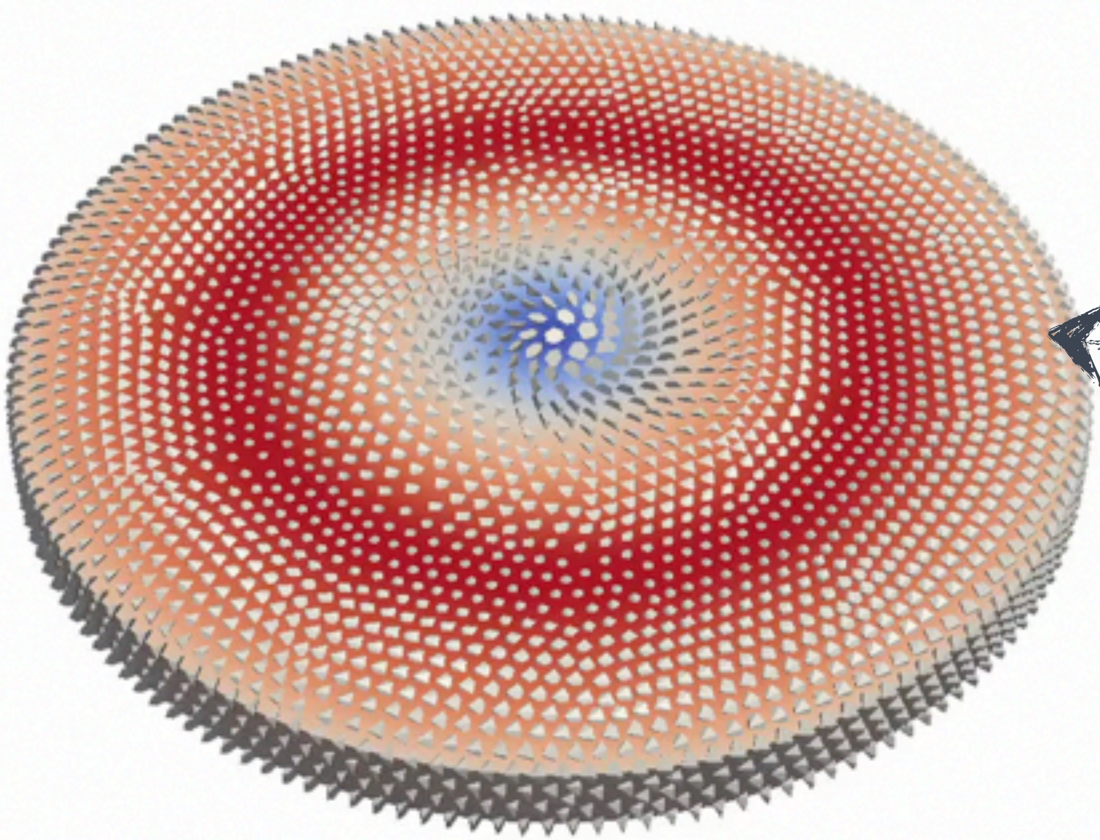

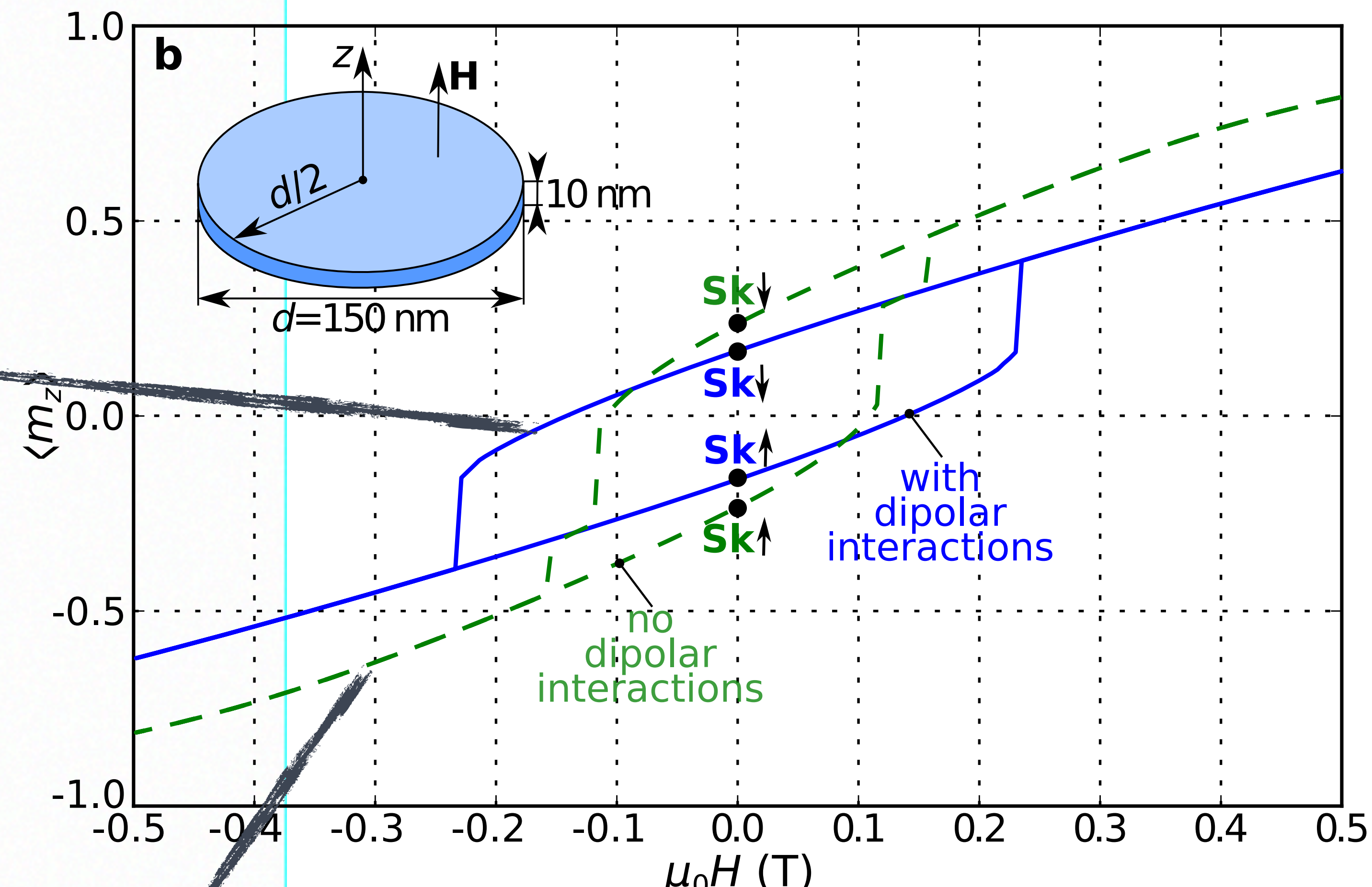

Hysteretic behaviour remains **in absence of** magnetocrysralline anisotropy and dipolar-based shape anisotropy, suggesting the existence of Dzyaloshinskii-Moriya based shape anisotropy.

REVERSAL MECHANISM

- Skyrmionic texture core reverses **via Bloch point occurrence and propagation**.
- Reversal from core down to core up.
- External field reduced abruptly from -210 mT to -260 mT.
- Magnetisation dynamics recorded for 1 ns.

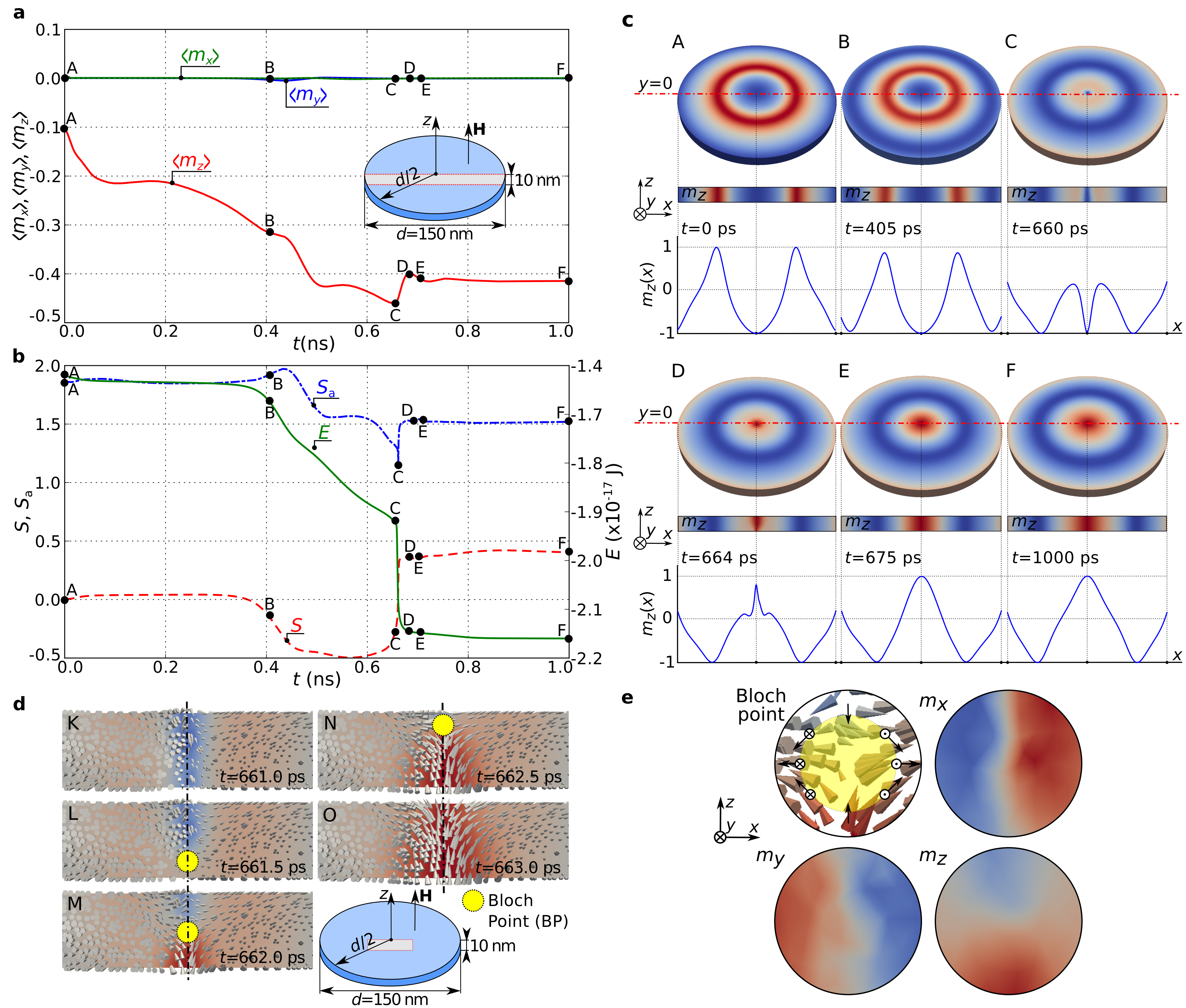

Liu, Y., Du, H., Jia, M., & Du, H. (2015), Physical Review B, 91, 094425.

REVERSAL MECHANISM

1. Core shrinks
2. Profile lowers
3. Core reverses
4. Size increases to adapt to the size of nanostructure.

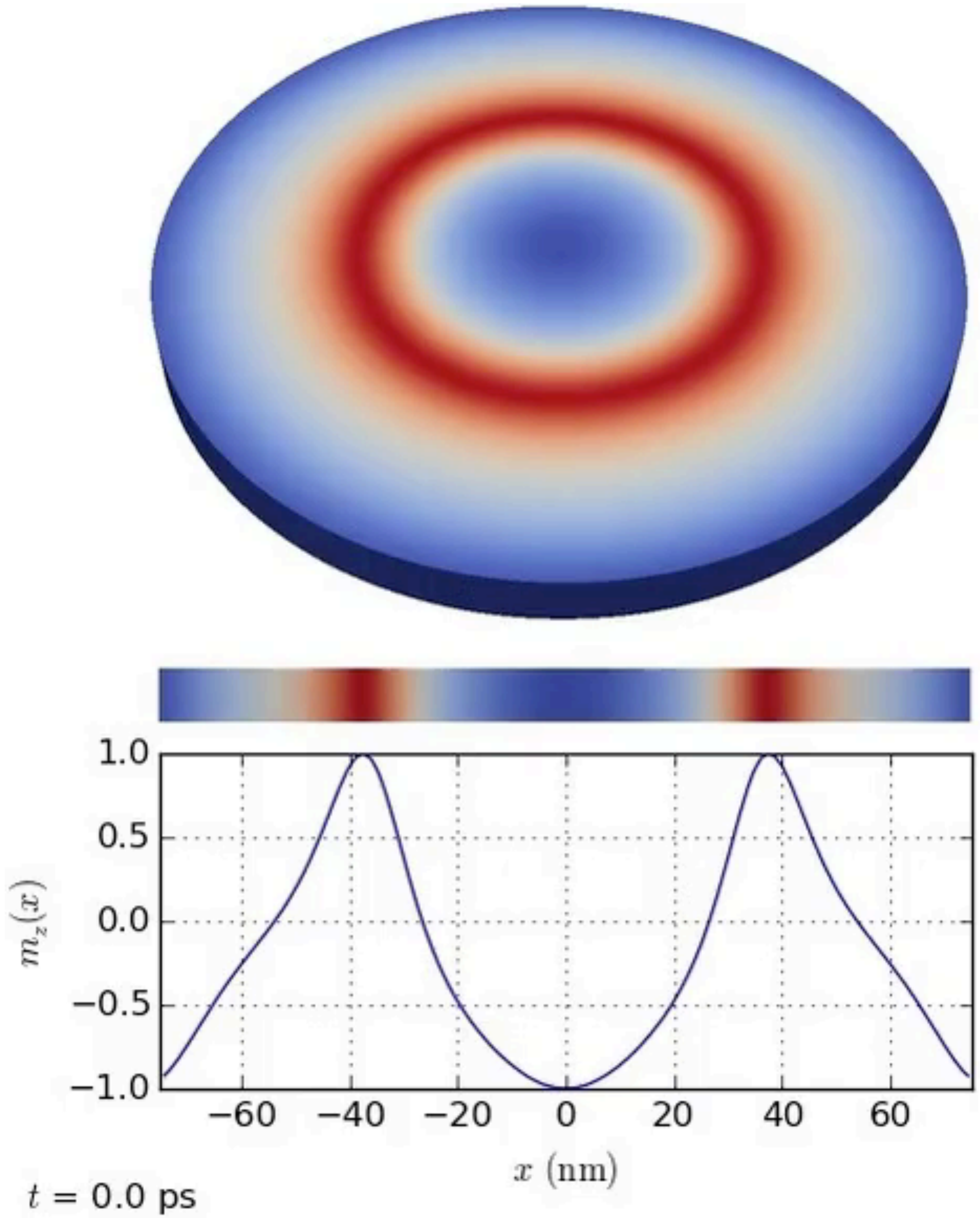

CORE REVERSAL MECHANISM

Bloch Point (BP):

1. enters the sample at the top boundary,
2. propagates to the bottom boundary, and
3. leaves the sample.

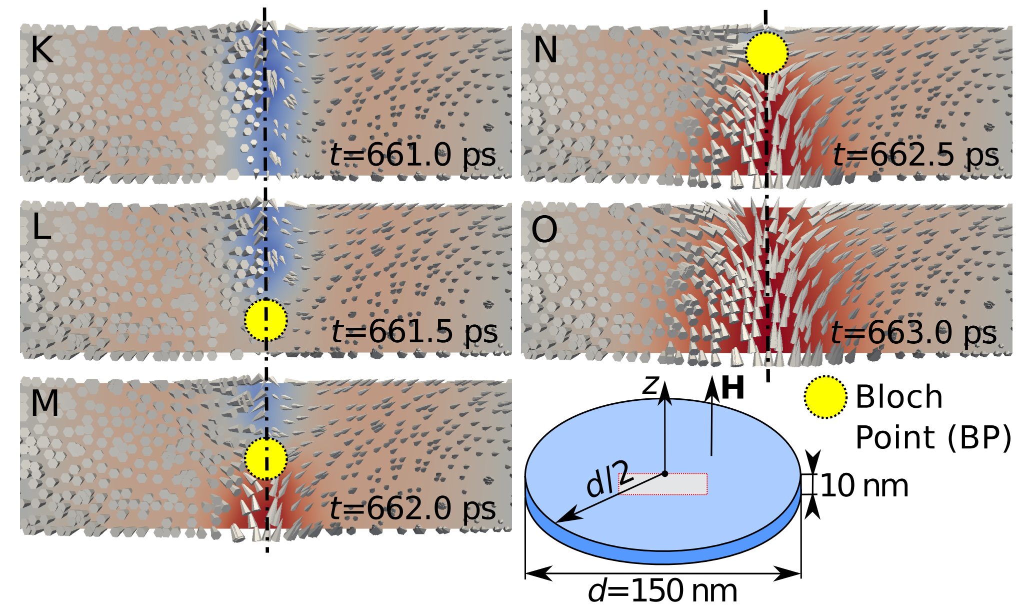

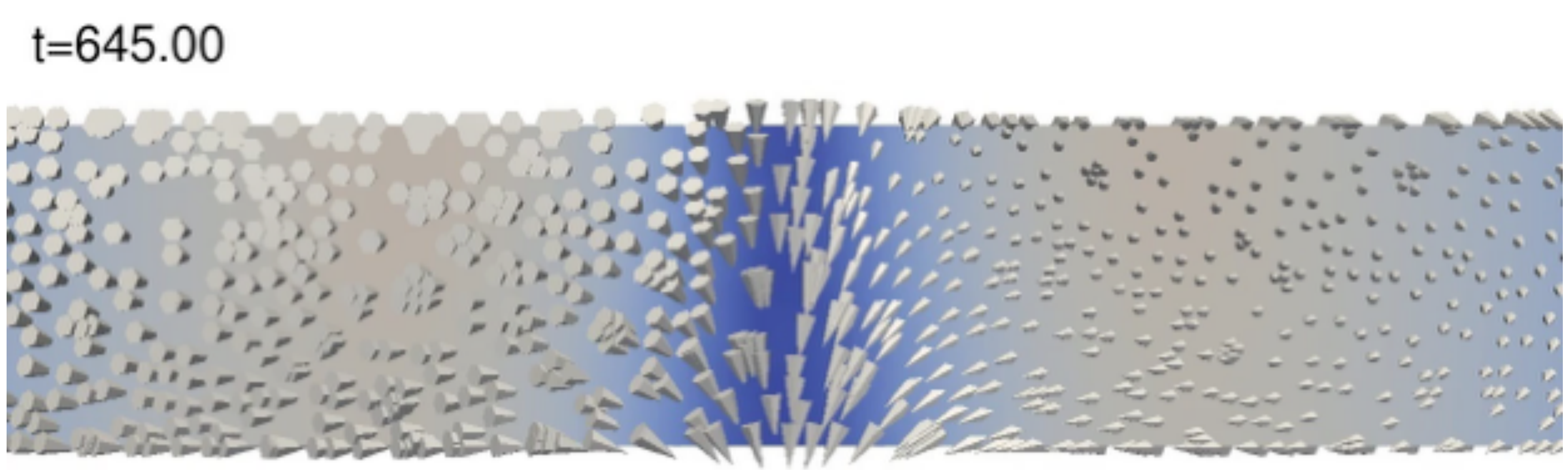

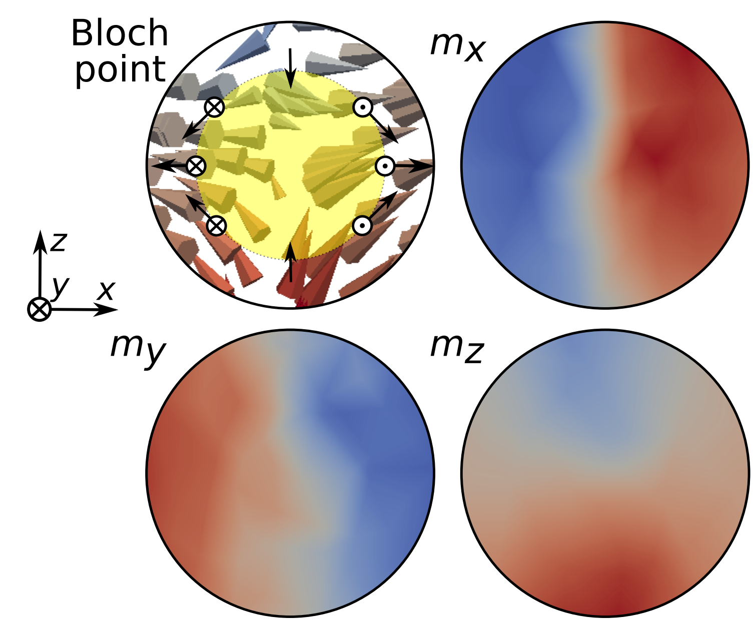

DIFFERENT BLOCH POINT PROPAGATION

- One may ask whether different BP propagation direction is allowed.
- This process is stochastic and depends on simulation parameters.
- We choose 0.35 for Gilbert damping.
- Bloch point structure changes.

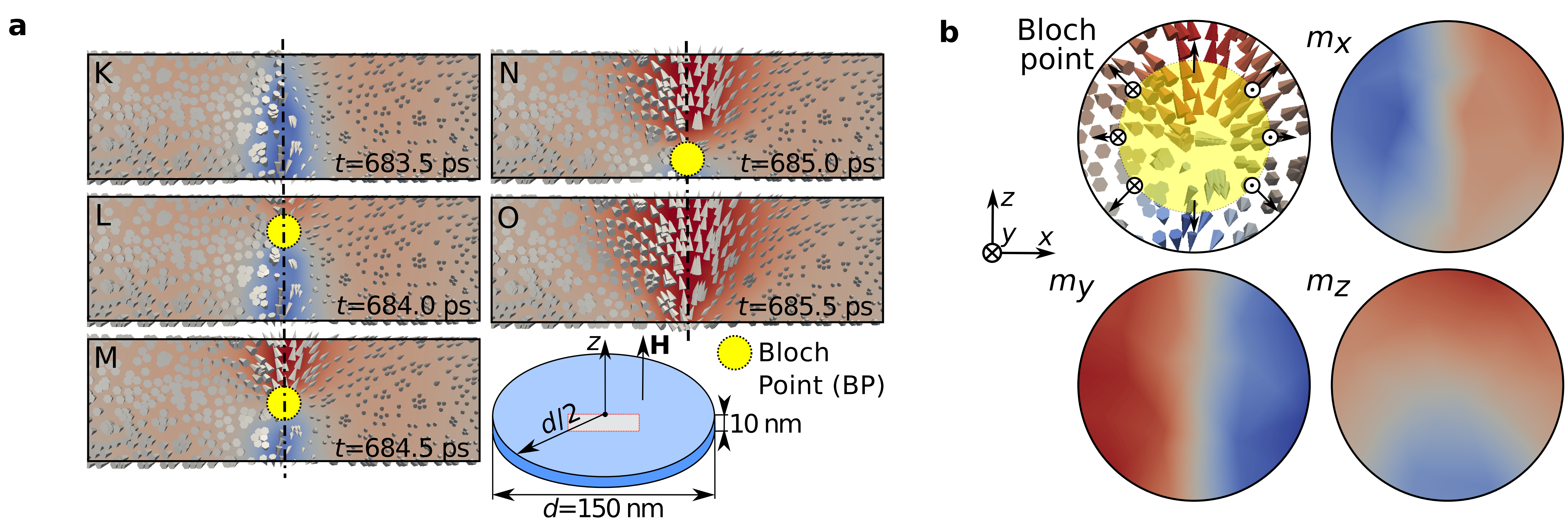

SUMMARY

- In finite size B20 helimagnetic samples skyrmionic textures are **ground state at zero field and in absence of magnetocrystalline anisotropy.**
- Skyrmionic textures occur in a much **wider range** of external field values.
- Demagnetisation energy and magnetisation variance in out-of-plane direction crucial for the stability.
- **Bistability**: Two energetically equivalent configurations with different core orientation identified .
- **Writability**: Skyrmionic textures undergo **hysteretic behaviour** when the core orientation is changed using an external field.
    - Large hysteresis identified in absence of magnetocrystalline and dipolar-based shape anisotropies, suggesting the existence of **DMI-based shape anisotropy.**
- Skyrmionic textures reverse via **Bloch-point occurrence and propagation.**
- Results **fully scalable** for helimagnetic materials with different helical period.
- Presented stable skyrmionic textures could be used for **hosting the information bit.**

- Paper: **Beg et al. Scientific Reports 5, 17137 (2015)**

- **Acknowledge** the financial support from the EPSRC's DTC grant EP/G03690X/1
- **Acknowledge** the help of Marijan Beg, Weiwei Wang, David Cortes, Rebecca Carey, Maximilian Albert, Dmitri Chernyshenko, Marc-Antonio Bisotti, Mark Vousden and Robert L. Stamps.

- **email**: mb4e10@soton.ac.uk

MICROMAGNETIC MODEL

- **Energy density**

$$w(\mathbf{m}) = \underbrace{A(\nabla \mathbf{m})^2}_{\text{exchange}} + \overbrace{D\mathbf{m} \cdot (\nabla \times \mathbf{m})}^{\text{DMI}} - \underbrace{\mu_0 M_\mathrm{s} \mathbf{m} \cdot \mathbf{H}}_{\text{Zeeman}} + \overbrace{w_\mathrm{d}}^{\text{demagnetisation}}$$

- **Effective field**

$$H_\mathrm{eff}(\mathbf{m}) = -\frac{1}{\mu_o M_\mathrm{s}} \frac{\delta w(\mathbf{m})}{\delta \mathbf{m}}$$

$$H_\mathrm{eff}(\mathbf{m}) = \underbrace{\frac{2A}{\mu_0 M_\mathrm{s}} \nabla^2 \mathbf{m}}_{\text{exchange}} - \overbrace{\frac{2D}{\mu_0 M_\mathrm{s}} (\nabla \times \mathbf{m})}^{\text{DMI}} + \underbrace{\mathbf{H}}_{\text{Zeeman}} + \overbrace{\mathbf{H}_\mathrm{d}}^{\text{demagnetisation}}$$

- **LLG equation**

$$\frac{\partial \mathbf{m}}{\partial t} = \underbrace{\gamma^* \mathbf{m} \times \mathbf{H}_\mathrm{eff}}_{\text{precession}} + \overbrace{\alpha \mathbf{m} \times \frac{\partial \mathbf{m}}{\partial t}}^{\text{damping}} + \underbrace{u(|\mathbf{m}| - 1)V(\mathbf{m})}_{\text{norm correction}}$$

DEMAGNETISATION

- **Magnetic scalar potential**

$$\phi(\mathbf{r}') = \frac{M_\mathrm{s}}{4\pi}\left(\underbrace{-\int_\Omega \frac{\nabla\cdot\mathbf{m}(\mathbf{r}')}{||\mathbf{r}-\mathbf{r}'||}\,\mathrm{d}V}_{\text{volume term}} + \overbrace{\int_{\partial\Omega} \frac{\mathbf{m}(\mathbf{r}')\cdot\mathbf{n}}{||\mathbf{r}-\mathbf{r}'||}\,\mathrm{d}S}^{\text{surface term}}\right)$$

- **Effective (demagnetisation) field**

$$\mathbf{H}_\mathrm{d}(\mathbf{r}) = -\nabla\phi(\mathbf{r})$$

- **Demagnetisation energy density**

$$w_\mathrm{d} = -\frac{1}{2}\mathbf{H}_\mathrm{d}\cdot\mathbf{m}$$